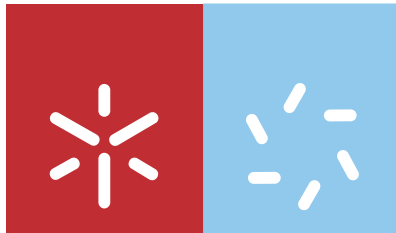


Universidade do Minho
Escola de Ciências

Filipa Oliveira Gomes

Bone Cements – development of partially degradable ionomer cements.



Universidade do Minho

Escola de Ciências

Filipa Oliveira Gomes

**Bone Cements – development of partially
degradable ionomer cements.**

Dissertação em Técnicas de Caracterização e Análise Química

Trabalho realizado sob a orientação de:

Supervisor: Professor Doutor Rui Luís Gonçalves dos Reis

Co-supervisor: Doutor Ricardo Alexandre Rodrigues Pires

**Orientador do Departamento de Química: Doutora Maria
Isabel Pontes Correia Neves**

Nome: Filipa Oliveira Gomes

Endereço eletrónico: figs8@hotmail.com

Telefone: 914192367

Número do Bilhete de Identidade: 13249166

O título da tese: **“Bone Cements – development of partially degradable ionomer cements.”**

Orientadores

Supervisor: Professor Doutor Rui Luís Gonçalves dos Reis

Co-supervisor: Doutor Ricardo Alexandre Rodrigues Pires

Orientador do Departamento de Química: Doutora Maria Isabel Pontes Correia Neves

Mestrado em Técnicas de Caracterização e Análise Química

É AUTORIZADA A REPRODUÇÃO PARCIAL DESTA TESE APENAS PARA EFEITOS DE INVESTIGAÇÃO, MEDIANTE DECLARAÇÃO ESCRITA DO INTERESSADO, QUE A TAL SE COMPROMETE.

Universidade do Minho, 29-09-2011

Assinatura:

“Quero dedicar a minha tese a duas pessoas muito importantes para mim: à minha mãe que passou momentos muito complicados durante o meu Mestrado e que continuou a lutar devido à sua força e à minha madrinha que foi o meu pilar a todos os níveis principalmente a nível emocional, sem este pilar tudo seria muito complicado.”

Acknowledgments

Gostaria de agradecer ao Professor Rui Reis por me ter dado a oportunidade de desenvolver a minha tese de mestrado no centro de excelência em biomateriais, biodegradáveis e biomiméticos (3B's). Agradeço também a disponibilidade demonstrada e as ideias/opiniões sugeridas ao longo da tese. É muito gratificante trabalhar num grupo com um nível tão elevado de conhecimento e com pessoas de diferentes nacionalidades e áreas.

Agradeço também ao Doutor Ricardo Pires pelo planeamento do trabalho e pelo apoio nas várias etapas. É gratificante encontrar uma pessoa com humildade, alegria e vontade de trabalhar e ajudar como o Doutor Ricardo Pires. Muito obrigada pela compreensão e pela motivação, foi uma das pessoas mais importantes ao longo deste trabalho.

Gostaria de agradecer à minha orientadora da Universidade do Minho, a Professora Isabel Neves, pela sua disponibilidade e conhecimento sobre esta área de estudo. Decidi fazer a minha tese na área dos materiais devido ao incentivo e entusiasmo que a Professora Isabel Neves demonstrou.

Agradeço à Doutora Elsa Ribeiro pela ajuda nas análises de SEM e EDS e pela discussão dos resultados obtidos e também ao Doutor Stanislav Ferdov pela ajuda nas análises de XRD.

Quero deixar o meu agradecimento ao grupo dos 3B's em geral e especialmente a algumas pessoas que me marcaram pela discussão de temas relacionados com a minha área e também sobre outros assuntos mas sobretudo pela amizade.

Agradeço particularmente à Maria que dispensou muito do seu tempo para me ensinar e pela preocupação demonstrada sobre o meu trabalho.

Aos meus colegas e professores de Mestrado, muito obrigada pela amizade e pelo conhecimento que adquiri.

Um agradecimento especial a toda a minha família principalmente ao meu pai por toda a força e inteligência que demonstrou no decorrer do meu trabalho. Mesmo com todas as adversidades nunca demonstreste fraqueza, obrigada pela força pai! Quero agradecer ao meu irmão o facto de sempre poder contar com ele, apesar de estar a viver em França.

As pessoas que mencionei contribuíram de forma diferente para o meu trabalho mas todas juntas foram essenciais para o resultado final.

Abstract

The first glass-ionomer cement (GIC) was developed by *Wilson and Kent* in 1971. GICs are usually prepared through the mixing of a fluoroaluminosilicate glass powder, polyacrylic acid (PAA) and water. The PAA attacks the glass particles that leach some of its cations (e.g. Al^{3+} and Ca^{2+}) to the cement matrix. These cations cross-link the PAA chains yielding the final cement structure. GICs possess as main advantage the ability to bind to hydroxyapatite present in the dentin and bone. These systems have been mainly used in the dentistry field (non-systemic application). Applications that induce a systemic uptake of the cement components (e.g. bone cements) have been discarded due to the presence of aluminium (a known neurotoxin) on the GIC formulations.

The present thesis targets the development of new glass-ionomer cement (GIC) formulations with potential to be applied as bone cements. To this purpose, new aluminium-free glass compositions of general formula $0.340\text{SiO}_2 : 0.300\text{ZnO} : (0.250-x-y)\text{CaO} : x\text{SrO} : y\text{MgO} : 0.050\text{Na}_2\text{O} : 0.060\text{P}_2\text{O}_5$ (where x and $y = 0.000$ or 0.125) were synthesised and tested in the formulation of GICs through their mixing with PAA and water. The different parameters that influence the GIC mechanical performance (e.g. glass particle size, molecular weight of PAA, proportion of the constituents, etc.) were optimized. The GIC prepared with the developed glass compositions were *in vitro* tested for their bioactivity. To this purpose, GIC samples were immersion in SBF and their ability to form a surface apatite layer was evaluated by: 1) determination of the concentration of the calcium and phosphorous in the SBF (executed by ICP); 2) quantification of the calcium and phosphorous present at the surface of the cements (executed by EDS) and 3) morphological analysis (executed by SEM). Micro-CT was also used to evaluate the spatial distribution of the polymeric and inorganic phases. Finally, in an attempt to enhance the GIC biodegradability it was incorporated starch in the cement formulations, at different weight percentages (5% and 25%).

The results obtained under this thesis proved the suitability of some of the developed glass compositions (e.g. $0.34\text{SiO}_2 : 0.30\text{ZnO} : 0.125\text{CaO} : 0.125\text{SrO} : 0.05\text{Na}_2\text{O} : 0.06\text{P}_2\text{O}_5$) to prepare GICs in accordance with its use as bone cements, including: suitable mechanical performance (compressive strength, $\text{CS}=25$ MPa; compressive modulus, $\text{CM}=492$ MPa) for non-load bearing applications; bioactivity; and 35 % porosity. Moreover, after the 8th week of degradation under enzymatic medium it was detected reducing sugars in the degradation solutions of the starch-containing formulations confirming its biodegradation potential at a longer timeframe.

Resumo

O primeiro cimento de ionómero de vidro (GIC) foi desenvolvido por *Wilson e Kent* em 1971. Estes cimentos são normalmente preparados através de uma mistura de um pó de vidro geralmente fluoroaluminossilicatos com ácido poliacrílico (PAA) e água. O PAA ataca as partículas de vidro que liberta alguns dos seus catiões (e.g. Al^{3+} e Ca^{2+}) para a matriz do cimento que vão ligar-se às cadeias do PAA. Os cimentos possuem como vantagens a capacidade para se ligarem à hidroxiapatite presente nos dentes e ossos. Estes sistemas têm sido usados principalmente na área dentária (aplicações não sistémicas). Aplicações que induzem uma absorção sistémica dos componentes do cimento têm sido rejeitadas devido à presença de alumínio (uma neurotoxina conhecida).

A presente tese tem como principal objetivo o desenvolvimento de novas formulações de cimentos de ionómero de vidro para aplicação como cimentos ósseos. Para este propósito, foram sintetizadas novas composições de vidros sem alumínio com a fórmula geral $0.340\text{SiO}_2: 0.300\text{ZnO}: (0.250-x-y)\text{CaO}: x\text{SrO}: y\text{MgO}: 0.050\text{Na}_2\text{O}: 0.060\text{P}_2\text{O}_5$ (onde x e $y = 0.000$ ou 0.125) e utilizadas na formulação de cimentos através da mistura com PAA e água. Os parâmetros que influenciam a performance mecânica dos cimentos (e.g. tamanho de partícula, peso molecular do PAA, proporção dos constituintes, etc.) foram otimizados. Os cimentos foram analisados *in vitro* para obter informação acerca da sua bioactividade. Para este estudo, amostras de cimentos foram imersas em SBF e a sua capacidade de formar uma superfície de apatite foi avaliada através da: 1) determinação da concentração de cálcio e fósforo presente em SBF (efetuado por ICP); 2) quantificação de cálcio e fósforo presente na superfície dos cimentos (efetuado por EDS); 3) análise morfológica (efetuado por SEM). Micro-CT foi utilizado para avaliar a distribuição de fases poliméricas e inorgânicas. Finalmente, para obtenção de cimentos biodegradáveis foi incorporado amido na sua formulação, com diferentes percentagens (5% e 25%).

Os resultados obtidos nesta tese demonstraram a possibilidade de algumas composições de vidro (e.g. $0.340\text{SiO}_2: 0.300\text{ZnO}: 0.125\text{CaO}: 0.125\text{SrO}: 0.050\text{Na}_2\text{O}: 0.060\text{P}_2\text{O}_5$) contribuírem para a preparação de cimentos com interesse para aplicação como cimentos ósseos, incluindo uma adequada performance mecânica (*Compressive strength*, $\text{CS} = 25 \text{ MPa}$; *Compressive modulus*, $\text{CM} = 492 \text{ MPa}$) para zonas de carga não permanente, bioactividade e 35 % de porosidade. Além disso, após a oitava semana de degradação em condições enzimáticas foram detetados açúcares redutores nas formulações contendo amido confirmando o seu potencial de biodegradação.

Index

Acknowledgments	iv
Abstract	v
Resumo	vii
List of Abbreviations	xiii
List of Figures	xv
List of Tables	xvii

Chapter I: General Introduction

1. General remarks	3
2. Bone regeneration/treatment	3
2.1 Bone – What is it?	3
2.2 Constitution of bone	4
2.3 Mechanical properties of bone	5
2.4 Bone repair	7
2.5 Self regeneration of bone	9
3. Biomaterials relevant to bone regeneration/repair	9
3.1 Ceramic-based biomaterials	12
3.2 Biocompatibility and bioactivity	16
3.3 The relevance of biodegradability	16
4. Glass ionomer cements (GICs)	18
4.1 The development of GICs	18
4.2 The importance of glass composition	19
4.3 Methodologies to synthesize the glass component	20
4.3.1 Melt-quenching methodology	20
4.3.2 Sol-gel methodology	20
4.4 The polymeric component	22
4.5 GIC curing reactions	22
4.6 Properties, applications and importance of GICs and its constituents	23
4.6.1 Properties of GICs	23
4.6.2 Applications of GICs	25
4.6.3 Biocompatibility of GICs	25
4.6.4 The importance of GIC cations in the regeneration of tissue	25
a) Aluminium and its toxicity	26
b) Other relevant cations	27
Bibliography	30

Chapter II: Materials and Methods

1. Materials	39
2. Materials synthesis and processing	40
2.1 Glass synthesis	40
2.2 Cement preparation	41
3. Characterization methodologies	42
3.1 Mechanical performance under compression loading	42
3.2 Fourier Transform Infrared Spectroscopy	43
3.3 X-ray powder Diffraction	43
3.4 Scanning Electron Microscopy	44
3.5 Micro-Computed Tomography	44
3.6 Water uptake and weight loss	45
3.6.1 Water uptake	45
3.6.2 Weight loss	46
4. Bioactivity assays	46
4.1 Preparation of Simulated Body Fluid and the cements samples	46
4.2 Bioactivity assay	47
4.3 Analysis of calcium and phosphorous concentration by inductive coupled plasma – optical emission spectroscopy	48
4.4 Energy-dispersive X-ray spectroscopy	48
5. Degradation studies	49
5.1 Enzymatic degradation – reducing sugars	49
6. Statistical methods	50
6.1. Dixon test (Q-test)	50
6.2. Normality test	51
6.3. t-test	52
Bibliography	53

Chapter III: Aluminum-free glass ionomer bone cements with enhanced bioactivity and biodegradability

Abstract	58
Keywords	58
1. Introduction	59
2. Materials and methods	60
2.1 Materials – glass synthesis	60
2.2 Cement preparation	61

2.3 Glass and cement characterization	61
2.3.1 X-ray diffraction	61
2.3.2 Fourier Transform Infrared spectroscopy	61
2.3.3 Mechanical testing	61
2.4 Bioactivity tests	62
2.4.1 <i>In vitro</i> bioactivity	62
2.4.2 Inductive coupled plasma – optical emission spectroscopy	62
2.4.3 Energy-Dispersive x-ray Spectroscopy	62
2.4.4 Scanning Electron Microscopy	62
2.5 Water uptake and weight loss	63
2.6 Degradation tests	63
2.7 Micro-Computed Tomography	64
3. Results and discussion	64
3.1 Glass characterization	64
3.1.1 X-ray diffraction	64
3.2 Cement characterization	65
3.2.1 Chemical characterization	65
3.2.2 Mechanical testing	66
a) Influence of glass particle size and PAA molecular weight on the cement mechanical behaviour	66
b) Influence of the composition of each cement in the mechanical behaviour	67
3.2.3 In vitro bioactivity	68
3.2.4 3D distribution of glass, PAA and porosity of C5 cement	70
3.2.5 Water uptake and weight loss	71
3.3 Addition of starch to the cement formulation	71
3.3.1 Mechanical testing	71
3.3.2 3D distribution of the glass, polymers and porosity on the starch-containing cements	72
3.3.3 Water uptake and weight loss	72
3.3.4 Degradation tests	74
4. Conclusions	75
Bibliography	77
 Chapter IV: General conclusions & Future research	 81
Bibliography	84

List of Abbreviations

CM – Compressive Modulus

CPC – Calcium phosphate cement

CS – Compressive Strength

DNS – Dinitrosalicylic acid

ECM – Extra cellular matrix

EDS – Energy dispersive x-ray spectroscopy

FTIR – Fourier Transform Infrared Spectroscopy

GIC – Glass ionomer cement

ICP – Inductive Coupled Plasma

ICP-OES – Inductive Coupled Plasma – Optical Emission Spectroscopy

Micro-CT – Micro-Computed Tomography

Mw – Molecular weight

PAA – Polyacrylic acid

PBS – Phosphate Buffer Saline

RMGIC – Resin Modified glass ionomer cement

SBF – Simulated Body Fluid

SEM – Scanning Electron Microscopy

TCP –Tricalcium phosphate

UV-VIS – Ultraviolet visible

w/w – Weight/weight

WL – Weight loss

WU – Water uptake

XRD – X-ray Diffraction

List of Figures

Chapter I

Figure 1: Hierarchical structural organization of bone	4
Figure 2: Stages of mechanical deformation: the elastic range (E), the continuum damage mechanics range (CDM) and the fracture mechanics (FM)	6
Figure 3: (a) Primary and secondary mineralized tissue repair; (b) Primary and secondary bone remodelling	8
Figure 4: Structure of starch (amylose and amylopectin)	18
Figure 5: Sol-gel process	21
Figure 6: Polymers already tested in the development of GIC formulations	22
Figure 7: GICs curing reactions during the gelation stage	23
Figure 8: Aluminium inflammatory response of Al-based GICs resulting in an irregular density at the specific positions (arrowheads)	27

Chapter II

Figure 1: Illustration the melt quenching process	40
Figure 2: Glass powder preparation and sieving	41
Figure 3: Example of the preparation of a moulded cement formulation	41
Figure 4: Instron 5540, Universal mechanical testing machine	42
Figure 5: Preparation of the KBr pellets	43
Figure 6: Gold deposition, microscope chamber and overall view of SEM microscope	44
Figure 7: Micro-Computed Tomography equipment	45
Figure 8: ICP-OES analysis of the developed cements	48
Figure 9: Carbon deposition of the analysed samples and EDS equipment	49
Figure 10: Scheme of normal distribution	51

Chapter III

Figure 1: X-ray powder patterns of the synthesised glass formulations	65
Figure 2: FTIR spectra of PAA, glass G5 and cement C5	65
Figure 3: Compressive modulus (CM) and compressive strength (CS) of the cements prepared with the different particle sizes of glass powder and PAA M_w s	66
Figure 4: Compressive modulus (CM) and compressive strength (CS) of the developed cements	67
Figure 5: EDS spectra the surface of cement C5 immersed in SBF for 7 and 14 days (spectrum of non-immersed cement shown as reference – 0 days)	69
Figure 6: SEM micrographs of cement C5 before and after immersion in SBF for 7 and	70

14 days

Figure 7: Compressive strength (CS) and compressive modulus (CM) for the cements as a function of the percentage of starch in the formulations **71**

Figure 8: Micro-CT bidimensional image and 3D image of C5 cement without starch and with 5 % and 25 % of starch **72**

Figure 9: Water uptake (WU) of the cements under PBS (a) and PBS + α -amylase (b) during 12 weeks **73**

Figure 10: Weight loss (WL) of the cements under PBS (a) and PBS + α -amylase (b) during 12 weeks **74**

Figure 11: Concentration of reducing sugars in the cements (with 5% and 25% of starch) after immersion in PBS during 12 weeks **75**

List of Tables

Chapter I

Table 1: Mechanical properties of cortical and cancellous bone	7
Table 2: Fields of knowledge relevant for the development of biomaterials	10
Table 3: Different areas where the use of biomaterials has been exploited	10
Table 4: Different types of biomaterials	11
Table 5: The main calcium phosphates used in the biomedical field	14
Table 6: Applications of biodegradable biomaterials in biomedical devices	17

Chapter II

Table 1: Specifications of all reagents used for the glass and cement preparation	39
Table 2: Composition of the synthesized glasses formulations	40
Table 3: Ionic concentration of the human blood plasma and the SBF solution	46
Table 4: Quantities and sequence of the addition of each reagent in the protocol followed for the preparation of the SBF solution	47

Chapter III

Table 1: Composition of the synthesized glass formulations (mol %)	60
Table 2: Ca and P concentrations in the SBF solutions (after 7 and 14 days of immersion). Values are presented as percentage of the concentrations present in the original SBF, used as reference	68
Table 3: Ca/P ratio of all cements after 7 and 14 days	69

Chapter I

General Introduction

1. **G**eneral remarks

This thesis addresses developments and optimizations on glass-ionomer cements (GICs) targeting their application in the repair of bone. Under this perspective, this introductory chapter will comprise an initial section that includes a series of considerations on the bone tissue, namely, its structure, properties, repair steps and self-regeneration. Afterwards, it will be presented a section on the biomaterials relevant to the bone regeneration and repair, namely, the inorganic-based bone cements - the group of materials that present properties and characteristics more similar to the system under study. This section also includes relevant concepts in the biomedical field, such as, biodegradability and bioactivity. Finally, a third section will focus on the GIC system, its components, curing reactions, properties, applications, advantages and disadvantages.

2. **B**one regeneration/treatment

2.1 Bone – What is it?

Bone is one of the main constituents of the skeleton that acts as a support structure for the vertebrates. In the materials point of view, it has been considered as a heterogeneous bioceramic composite exhibiting variations on its chemical composition in between species. In fact the most noted differences in its mineral constitution are observed between two types of bones: rat and fish bone. It was also detected differentiated chemical composition in the skeletons of the hamster, monkey, pig, man and other vertebrates [1-5].

In order to better understand the relationships between bone chemical composition and its properties it is relevant to understand the mechanisms involved in bone related chemical processes, e.g. chemistry of calcification, bone as an ion reservoir, among others. Biltz and co-workers also concluded

that bone possesses chemical differences that are dependent on the age, exerted strength, metabolic activity and sex of the individual. Depending on these factors, it is observed a variation on the quantity of water and organic components present in the bone. In this perspective, it was also established a relationship between the bone water content and its degree of mineralization [3].

Each individual presents different types of bone within the body. The main differences are related with its density, from a more compact structure (cortical bone) to a less dense material (cancellous bone). Based in the study of the bone individual components it was concluded that its main properties (stiffness, elasticity, hardness and toughness) are derived from their combination in an heterogeneous structure [1]. It is also known that systematic loading affects bone mass and size. This is one of the reasons for the observed variations on bone density with the age of the individual [5].

2.2 Constitution of bone

Bone is a metabolically active tissue composed by a mineral and an organic phase that contribute to two thirds and one third of its weight, respectively [4]. As shown in Figure 1 the bone exhibits a structure that has elements of several length scales and which, together, perform various mechanical, chemical and biological functions, e.g. it acts as a support structure, reservoir of mineral ions, among others [6]

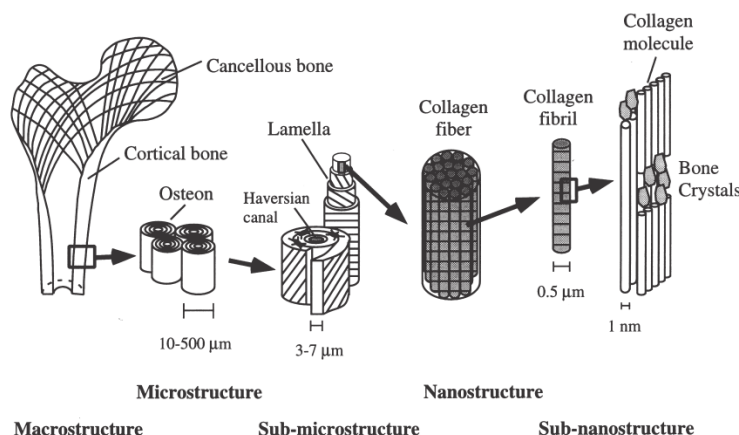


Figure 1: Hierarchical structural organization of bone.

Has stated before, bone is a heterogeneous bioceramic that combines an inorganic with an organic phase. In terms of its chemical composition, its main component is in the inorganic phase: carbonated hydroxyapatite (60-70 % w/w) of low crystallinity. The organic phase is mainly composed by fibrils of Type I collagen, although, other components are present, namely: growth factors and glycosaminoglycans. Finally, approximately 10 % of bone is composed by water [2].

The different types of bones (e.g. cortical or cancellous) are histologically different, although, their chemical composition is similar. Cortical bone represents, approximately, 80 % of the skeleton. It is dense and compact and possesses a high resistance to bending. Most of this type of bone is calcified and its main function is mechanical support and protection. Cancellous bone represents 20 % of skeletal mass and, approximately, 80% is found at the ends of long bones and in the interior of the vertebrae and pelvis. It is less dense, more elastic, and has a higher turnover rate than compact bone [7].

Bone is also constituted by cells. In fact there are three main types of cells in the bone tissue: osteoblasts, osteocytes and osteoclasts. Osteoblasts are the cells responsible for synthesis and deposition of minerals and, therefore, the mineralization of bone extracellular matrix. During their activity osteoblasts can become isolated in a cavity surrounded by bone matrix as a result of the deposition of minerals. Under these circumstances they differentiate into osteocytes, one of the most abundant types of cell in bone. Finally, osteoclasts are responsible for the bone remodelling process and their principal function is to resorb mineralized bone [8].

2.3 Mechanical properties of bone

In the context of mechanical evaluation it is relevant to describe the different data that can be extracted from the uniaxial mechanical tests. In this perspective, Figure 2 presents a stress-strain curve obtained from a mechanical test. The curve is the result of applied stress and the following data can be collected [1]:

- Beginning of the elastic behaviour;
- Elastic range;
- Range of plastic deformation;
- Breaking point;
- Amount of energy absorbed by the material;
- Elastic modulus (measuring the slope at the elastic range).

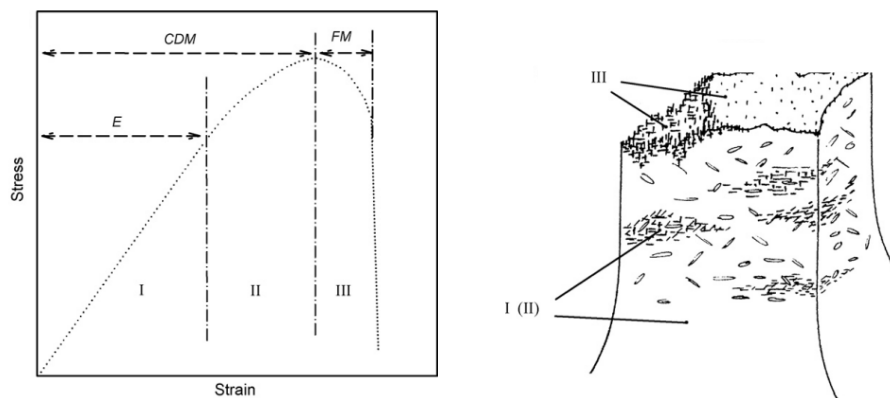


Figure 2: Stages of mechanical deformation: the elastic range (E), the continuum damage mechanics range (CDM) and the fracture mechanics (FM).

The mechanical behaviour of a material can be divided in three phases (I, II and III). Under I (the elastic regime) the material deforms reversibly and only residual damage occurs. Phase II corresponds to the plastic regime where the material absorbs enough energy to develop microcracks. In phase III it occurs mechanical failure and the amount of energy that the material is able to absorb reduces drastically.

Under mechanical loading, the bone can suffer of different types of ageing that can lead to fractures. These ageing mechanisms can be derived from creep (with prolonged load) or fatigue (repetitive) [9]. It has become recently clear that bone and other biological hard tissues show weak interlamellar interfaces, which are able to absorb energy and/or divert a crack. In this way, bone has a

limited capacity to detain the onset and growth of fracture. Furthermore, it is now increasingly clear that initiation of cracks in biomineralized tissues is far less important than their propagation since biological tissues use a number of processes (e.g. crack diversion/deflection, fibre pull-out, crack and/or matrix bridging) to increase the required amount of energy for fracture to occur [9].

The mechanical behaviour of bone depends on its type (cortical or cancellous). Additionally, as with any biological sample its variability is significant representing a reasonably large interval of expectable values. Table 1 resumes the most relevant mechanical properties of the two main types of bone.

Table 1: Mechanical properties of cortical and cancellous bone [10].

Property	Cortical bone	Cancellous bone
Compressive strength (MPa)	100-230	2-12
Flexural, tensile strength (MPa)	50-150	10-20
Strain to failure (%)	1-3	5-7
Young's (tensile) modulus (GPa)	7-30	0.5-0.05

2.4 Bone repair

When the ends of fractured bone are held in place, there are two types of primary mineralized tissue healing that can occur: gap repair and contact repair. In gap repair, healing begins by the formation of blood vessels and connective tissue fills the empty spaces. After 2 weeks osteoblasts fill the gaps in the tissue by secreting osteoid. Upon 10 more days osteoids became mineralized and the osteoblasts that remained in the matrix become entrapped. The new bone acts as a scaffold for remodelling promoted by osteoclasts and osteoblasts. In contact repair, there is no gap between the bone ends, although, necrotic bone must be removed before new bone can be deposited to repair the fracture. Osteoclasts are responsible to resorb the necrotic bone. Afterwards, osteoblasts attach to the tissue matrix, creating a ruffled cell border between the

cell and the bone surface promoting mineralization of the bone and subsequent re-linking of the bone surfaces.

In bone repair, secondary healing occurs when bones are not rigidly supported after the injury. The first step is to create an ECM-rich bridge to support the fracture and the unstabilized mineralized tissue will undergo secondary repair. Most compact bone surfaces that make up the outer layer are covered by osteoblasts that promote mineralization. The wound site will re-gain some mechanical strength after 4 days of healing (Figure 3 (a)).

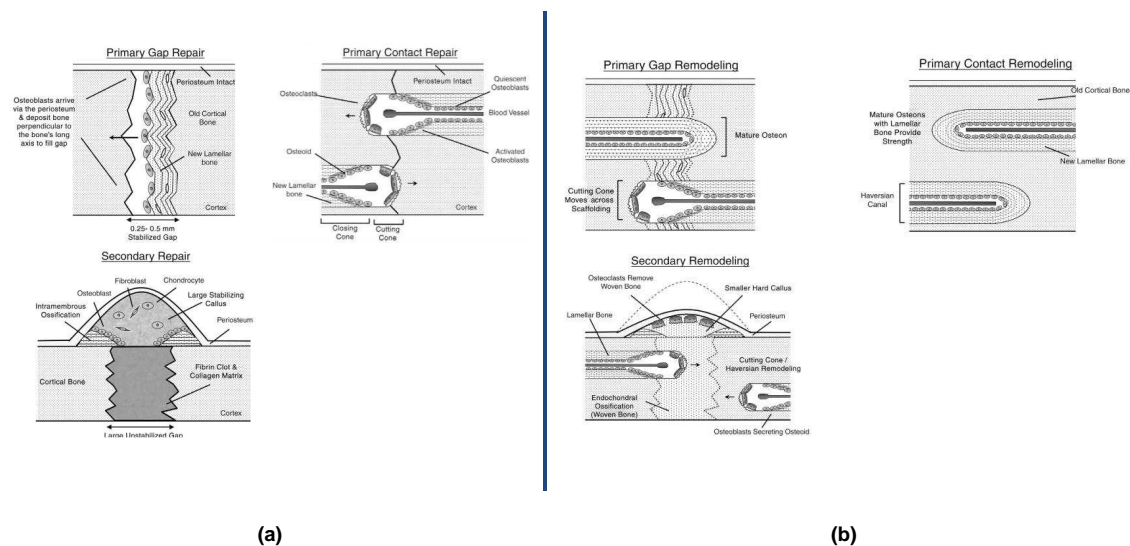


Figure 3: (a) Primary and secondary mineralized tissue repair; (b) Primary and secondary bone remodelling.

The mineralized bone remodelling is a dynamic process and occurs throughout the life of the individual. It produces new bone to be able to handle the demands of mechanical stresses. Primary gap remodelling also occurs during the repair process and lamellar bone (that presents collagen in a lamellar structure) is used as scaffold. After ca. 4 weeks osteogenesis stops leaving behind a vascularized cavity called an osteon that runs parallel to the long axis. A greater ultimate strength is obtained when a more osteons cross the injury site.

In primary gap healing, remodeling is important for restoring tissue strength. However, in primary contact healing, remodeling is coupled to the repair

process. During contact remodeling, the cutting cones mature, depositing lamellar bone centripetally to form ring-shaped structures.

The remodelling can last until 6 months and the healed bone is similar to the non-injured tissue in terms of robustness, although, it appears less organized. In this step it is also required to remove the excess of callus produced during the bone repair, being this step one of the main differences between the two reparation processes: primary and secondary. This callus removal is executed by the osteoclasts (Figure 3 (b)) [11].

2.5 Self-regeneration of bone

Bone is a dynamic tissue that is being formed and resorbed in a continuous cycle. These activities are executed in response to hormonal and physical factors. Bone is able to regenerate under different circumstances, e.g. when a fracture occurs in the bone. Unfortunately, this ability for self-regeneration is limited when the size of the trauma is too large. These cases are known as critical size defects due to the inability of the bone to self-regenerate. In order to repair these defects it is mandatory to execute a bone replacement. This can be achieved using a series of different biomaterials [12].

3. **B**iomaterials relevant to bone regeneration/repair

A biomaterial is a synthetic or natural material used to: replace part of living tissue; or to restore a specific function of the living tissue. From this definition it is clear to understand that the development of biomaterials usually comprise different fields of knowledge (Table 2), from materials science, biology and medicine. The effective influence of these areas is dependent on the specific tissue that is targeted and the function that the biomaterial is required to execute. In Table 3 is shown the application areas of the biomaterials. These can range from assistance in the diagnostic and treatment of diseases to tissue replacement or correction and improvement of tissue function [13].

Table 2: Fields of knowledge relevant for the development of biomaterials [13].

Knowledge domain	Examples
Materials science and engineering	Structure-property relationship of synthetic and biological materials including metals, ceramics, polymers, composites, tissues (blood and connective tissues), etc.
Biology and physiology	Cell and molecular biology, anatomy, animal and human physiology, histopathology; experimental surgery, immunology, etc
Clinical sciences	All the clinical specialties: dentistry, maxillofacial, neurosurgery, obstetrics and gynecology, ophthalmology, orthopaedics, otolaryngology, plastic and reconstructive surgery, thoracic and cardiovascular surgery, veterinary medicine, and surgery, etc.

Table 3: Different areas where the use of biomaterials has been exploited [13].

Area of intervention	Examples
Replacement of diseased or damaged part	Artificial hip joint, kidney dialysis machine
Assist in healing	Sutures, bones plates, and screws
Improve function	Cardiac pacemaker, intraocular lens
Correct functional abnormality	Cardiac pacemaker
Correct cosmetic problem	Augmentation mammoplasty, chin augmentation
Aid to diagnosis	Probes and catheters
Aid to treatment	Catheters, drains

The specific biological responses that the different biomaterials promote when in contact with the cells and body fluids are an important factor to be considered when designing new biomaterials [14-16]. In fact, the biomaterial-cell interaction is governed by the biomaterial surface and composition. Moreover, the different biomaterial properties (e.g. mechanical, biocompatibility, etc.) are governing their application area.

Table 4: Different types of biomaterials [13].

Biomaterial	Advantages	Disadvantages	Examples
Polymers (nylon, silicone rubber, polyester, polytetrafluoroethylene, etc.)	Resilient Easy to fabricate	Not strong Deforms with time, may degrade	Sutures, blood vessels, hip socket, ear, nose, other soft tissues, sutures
Metals (Ti and its alloys, Co-Cr alloys, stainless steels, Au, Ag, Pt, etc.)	Strong, tough, ductile	May corrode, dense, difficult to make	Joint replacements, bone plates and screws, dental root implants, pacer and sutures wires
Ceramics (aluminium oxide, calcium phosphates including hydroxyapatite, carbon)	Very biocompatible, inert, strong in compression	Brittle, not resilient, difficult to make	Dental; femoral head of hip replacement, coating of dental and orthopaedic implants
Composites (carbon-carbon, fibre-reinforced bone cement)	Strong, tailor-made	Difficult to make	Joint implants, heart valves

As can be seen from Table 4, in general, biomaterials can be produced from a variety of different materials (e.g. polymers, metals, ceramics and composites), although, their selection is dependent on their specific properties. As an example, while ceramics, metals and composites are usually used to repair

tissues that require high mechanical modulus, polymers that present lower mechanical modulus are usually selected to develop biomaterials for the repair or substitution of soft tissue. In the following subsection it will be presented examples of ceramic-based biomaterials due to the fact that is the type of biomaterials that presents more similarities with the systems studied under this thesis (GICs).

3.1 Ceramic-based biomaterials

Calcium phosphate cements (CPCs) were introduced in the field of bioceramics more than two decades ago and represented a real change in the medical applications. The possibility to have an injectable material with mouldable behaviour represented benefits for several clinical applications, e.g. minicracks, maxillofacial deformities and defects, vertebroplasty, among many others.

The formation of CPCs is based on the combination of one or more calcium orthophosphates. These phosphates are mixed with the liquid phase forming a paste that is able to set and harden after being implanted within the body. The CPC setting occurs through dissolution and precipitation of its components throughout the curing reactions. Its hardening is based on the entanglement of the precipitated crystalline phases. The most stable crystalline phases formed during the CPC curing are hydroxyapatite and brushite at $\text{pH} > 4.2$ and $\text{pH} < 4.2$, respectively [17].

The understanding of the mechanism of interaction of CPCs, allows accessing their long-term potential. It has been shown the occurrence of a gradual modification at the ceramic surface due to dissolution, precipitation and ion-exchange reactions. These events results in the production of a carbonate-containing, calcium-deficient hydroxyapatite with small crystal sizes. These changes are the beginning of a series of events that promotes bioactivity and that induces parallel reactions in cellular activity, bone mineralization and organic matrix deposition.

Absorption of proteins and other biological molecules occurs and the surrounding cells attach to the CPC surface. All these phenomena lead to the gradual incorporation of the ceramic into the regenerated bone tissue. Calcium phosphate ceramics include several materials which differ not only in their chemical composition, but also in their specific surface area, macro- and microporosity and crystal structure. There are differences due to variations in the calcium to phosphate ratio; as examples, tricalcium phosphate, hydroxyapatite and tetracalcium phosphate have Ca/P ratios of 1.50, 1.67 and 2.00 respectively, and there are other materials with ratios in between these (Table 5). Furthermore, hydroxyl ions may be missing from the structure, as in oxyhydroxyapatite, and other trace ions may be present. The importance of these compositional variations is not merely academic but they affect the biological response [18].

Table 5: The main calcium phosphates used in the biomedical field [8].

Compounds	Chemical Formula	(Ca/P) Molar Ratio	Abbreviation
Precipitated CaP			
Dicalcium phosphate	CaHPO_4	1.00	DCP
Monocalcium phosphate monohydrate	$\text{Ca}(\text{HPO}_4)_2 \cdot \text{H}_2\text{O}$	0.50	MCPM
Dicalcium phosphate dihydrate (Brushite)	$\text{Ca}(\text{HPO}_4)_2 \cdot 2\text{H}_2\text{O}$	1.00	DCPD
Octacalcium phosphate	$\text{Ca}_8\text{H}_2(\text{PO}_4)_6 \cdot 5\text{H}_2\text{O}$	1.33	OCP
Precipitated hydroxyapatite (tricalcium phosphate)	$\text{Ca}_{10-x}(\text{HPO}_4)_x(\text{PO}_4)_{6-x}(\text{OH})_{2-x} \quad 0 \leq x \leq 2$	1.50-1.67	PHA
Amorphous calcium phosphate	$\text{Ca}_3(\text{PO}_4)_2 \cdot n\text{H}_2\text{O}$ $n = 3-4.5; 15-20 \% \text{H}_2\text{O}$	1.50	ACP
High-Temperature CaP			
Monocalcium phosphate	$\text{Ca}(\text{HPO}_4)_2$	0.50	MCP
α -Tricalcium phosphate	$\alpha\text{-Ca}_3(\text{HPO}_4)_2$	1.50	α -TCP
β -Tricalcium phosphate	$\beta\text{-Ca}_3(\text{PO}_4)_2$	1.50	β -TCP
Sintered hydroxyapatite	$\text{Ca}_5(\text{PO}_4)_3\text{OH}$	1.67	HA
Oxyapatite	$\text{Ca}_{10}(\text{PO}_4)_6\text{O}$	1.67	OXA
Tetracalcium phosphate	$\text{Ca}_4(\text{PO}_4)_2\text{O}$	2.00	TetCP

Different types of bone cements are available for filling bone defects originated by illness or traumatic accident. More recently, bone cements have been tested for tendon-bone healing. In this perspective, Osteocrete, a magnesium-based injectable bone cement, has been reported to possess tensile strength 3 times higher than the calcium-based CPCs in both tendon-bone attachments and bone-bone structures. It has also been shown to enhance the formation of bone callous in an osteotomy model when compared with CPCs. While these preliminary studies are encouraging, the ability of Osteocrete to improve the healing of the bone tissue has not been studied [19].

Synthetic hydroxyapatite is a calcium-phosphate bioceramic of general chemical formula $\text{Ca}_{10}(\text{PO}_4)_6(\text{OH})_2$. It has been tested in the development of different types of biomaterials mainly targeting the substitution/regeneration of bone. This approach follows a biomimetic path derived from the fact that hydroxyapatite is one of the main constituents of natural bone. In fact, the inclusion of hydroxyapatite in biomaterials usually enhances their bioactivity and biocompatibility [20-23]. The advances in the ceramic technology generated a significant number of ceramic materials for medical purposes. As an example, tricalcium phosphate (TCP) was first proposed in 1920 as a bioresorbable substance to fill bone defects. However, TCP is a weak ceramic, unable to sustain significant loading. The need for tougher and stronger ceramics was not met before 1965, when the fillers alumina-based materials were proposed for the substitution of hip joints. Zirconia and synthetic calcium phosphate ceramics (together with other calcium and/or phosphorus containing ceramics and glasses) were then proposed as alternatives to alumina and TCP, respectively. After roughly 100 years of clinical use, we come to the conclusion that there is, so far, no ceramic biomaterial able to create a strong and biologically relevant interface with bone. On the other hand, ceramics and glasses are able to promote direct bone-implant adhesion without soft tissue interlayer, although, their mechanical properties are not sufficient to allow their use in load-bearing applications [24].

3.2 Biocompatibility and bioactivity

Biocompatibility is defined as the ability of a material has to give an appropriate response to a specific application (this definition was established by consensus among the specialists in the field of biomaterials, in a conference in Chester, UK. Williams 1987). Inevitably the introduction of a new material in the human body produces a specific response that depends on the composition of the biomaterial, shape, size, geometry and aspects of the organism/patient such as age, immunological sensitivity, health, local implant, among others. Therefore, it is difficult to mention what are the parameters that should be accounted to evaluate the biocompatibility of a specific material. Under this perspective each biomaterial should be evaluated according to the roles that it was designed to execute [25].

The bioactivity of a material is related with his ability to produce a chemical or biological response from the surrounding medium in order to promote tissue regeneration. A typical *in vitro* bioactivity test evaluates the ability of the biomaterial to form an apatite surface layer when in contact with simulated body fluid (SBF), a solution that presents the ionic concentrations similar to human blood plasma. The higher the ability of the biomaterial to form an apatite layer the higher is its bioactive potential [26]. As an example bioglass was the first successful glass to present bioactivity. It was first reported by Hench and co-workers in 1970s and was used clinically. The main application of these glasses is for replacement of the damaged tissue, as for example, treatment of facial bone injuries or benign bone tumours [27, 28].

3.3 The relevance of biodegradability

Biodegradable biomaterials are used in reconstructive surgery when the body itself has the capacity to self-regenerate the damaged tissue. Usually, a biomaterial to be used under this approach needs to present bioactivity and to promote tissue growth/regeneration. Upon application, the biomaterial start the degrade allowing the surrounding tissue to grow to the intervened area. The

correct matching between its degradation rate and the tissue growth/regeneration allows a complete regeneration of the damaged tissue upon full degradation of the biomaterial. Under this perspective it is of critical importance the non-toxicity of the degradation products. The first synthesized biodegradable biomaterial approved to be used in clinical applications (e.g. sutures) was the poly(glycolic acid) (PGA). With the progress of tissue engineering other biodegradable materials were developed (e.g. gellan gum, etc.) [29, 30]. The biodegradable biomaterials can be applied in the biomedical field in a diversified manner. In Table 6 it is presented examples of the targeted applications of biomedical devices produced using biodegradable biomaterials [8].

Table 6: Applications of biodegradable biomaterials in biomedical devices.

Application	Biomedical device
Adhesion and fixation of tissues	Suture, bone fixation material and adhesive
Support and reinforcement	Suture reinforcement material
Temporary substitutes for tissues	Substitute material for endocranium
Shape maintenance and isolation	Membrane for prevention of tissue adhesion
Securing space for tissue regeneration	Guided tissue regeneration, guided bone regeneration
Scaffold for tissue regeneration	Skin, cartilage, bone, blood vessel

A common approach to impart biodegradability to different biomaterials is the addition of starch. This methodology has been attempted in the development of bone cements [31, 32]. Starch is a glucose-based polymer created by the combination of two structures: amylose and amylopectin (Figure 4).

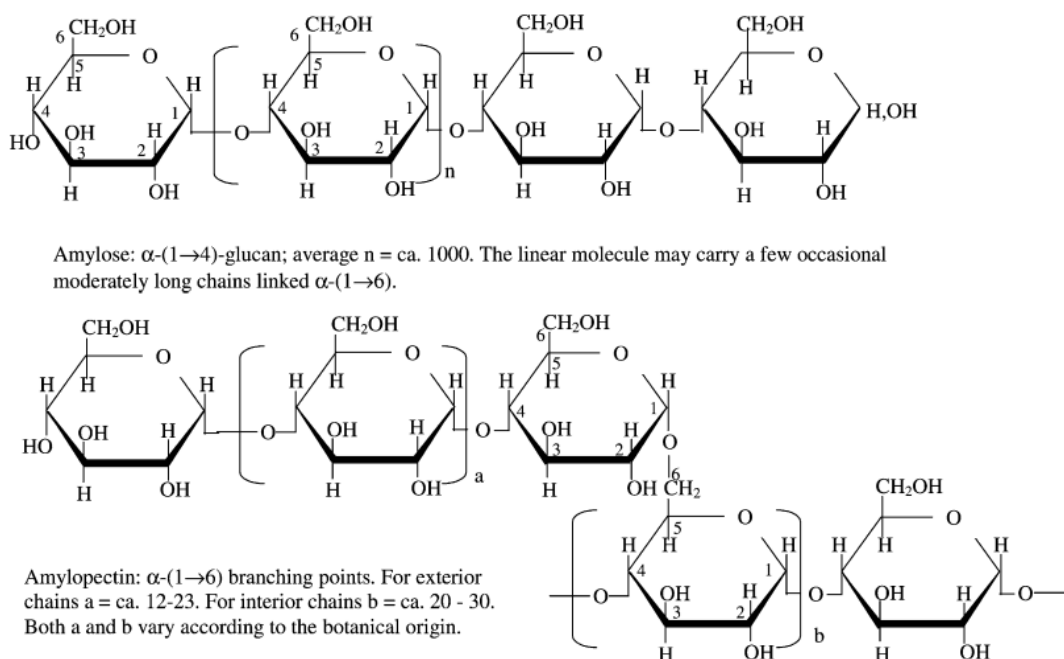


Figure 4: Structure of starch (amylose and amylopectin) [33].

Amylose is an essentially linear structure where the glucose units are joined by α (1 \rightarrow 4) glycosidic linkages. Amylopectin consists of linear α (1 \rightarrow 4) linked glucose chains including branched positions with α (1 \rightarrow 6) linkages every 24 to 30 glucose residues, on average [8].

One of the main advantages of including biodegradable starch in the formulation of biomaterials is the presence of α -amylase in the Human body that is specific for starch components. Additionally, its degradation products are not toxic and metabolized by the body.

4. **G**lass-ionomer cements (GICs)

4.1 The development of GICs

Wilson and Kent created the first conventional GICs combining a glass powder from the system $\text{SiO}_2\text{-Al}_2\text{O}_3\text{-CaO-CaF}_2$ with PAA, as a result of their pioneering work at the Laboratory of the Government Chemist, London, in the early 1970s [34-49]. The studied glasses became vulnerable to acid attack and

established a strong link with the acidic PAA [40]. Initial application of these GICs was in dentistry, as a colour matched alternatives to amalgam restoratives due to two main advantages: strong adhesion to dentin and ability to prevent caries in tooth structures [34, 50-52]. Research work during the following decades addressed their main disadvantages, namely, sensitivity to moisture during initial hardening; poor mechanical properties, among others [53]. Different optimizations introduced in the following decades resulted in the development of conventional GIC formulations that present enhanced mechanical performance, tuned curing time and reduced sensitivity to moisture. More significant modifications were promoted with the addition of UV-curable resins in the cement matrix. These resin-modified GICs present mechanical properties that overpass most of the conventional GICs, although, their anti-cariogenic potential was significantly reduced. In this sense, their properties, ease of moulding and ease of application, still makes conventional GIC as an extremely versatile solution for cementing a series of different biomaterials.

4.2 The importance of glass composition

The glass powder present in GIC formulations is usually composed by calcium fluoroaluminosilicates. This component has two main functions: 1) to act as a source of cations essential for the evolution of the cement curing reactions; and 2) to reinforce the final cement structure.

Within the typical glass systems used in GIC formulations it is possible to distinguish glass formers (e.g. SiO_2), glass modifiers (Ca^{2+}) and components with intermediate behaviour (e.g. Al_2O_3). The selection of components to be used in the glass formulation is dependent on several factors, including their influence in: the glass mechanical properties; the glass reactivity; and, most important, the glass basicity. In fact, the GIC curing is governed by acid-base reactions between an acidic polymer and a basic glass. In this sense, it is mandatory that the glass structure presents significant basicity. This basicity is usually conferred by the modifier cations.

4.3 Methodologies to synthesize the glass component

4.3.1 Melt-quenching methodology

Melt-quenching methodology is a high temperature process that involves the melting of the whole glass formulation and its subsequent fast decrease of temperature below the glass transition (T_g). This procedure induces the formation of the short to medium range order that is characteristic of glasses. The timeframe of the temperature reduction is so short that it does not allow the formation of long-range structural ordering. In general, glasses produced by this methodology present higher stability when compared with other glass preparation methods, e.g. sol-gel. Additionally, melt-quenched glasses usually promote the improvement of the mechanical behaviour of GIC compositions [14].

One of the main drawbacks of the melt-quenching technique is the fact that not all the compositions produce a melt. Depending on the glass compositions the melting temperature of the formulation is, in some cases, difficult to achieve with laboratory furnaces. Additionally, in the quenching step it is important to reach the appropriate temperature decrease rate that is also dependent on the composition. This should be fast enough to limit nucleation and to inhibit crystallization of the structure, although, nucleation and crystallization rates are also dependent on the composition. In fact, some formulations present a very high nucleation and crystallization rate and the production of pure glass phases is difficult. In these cases the melt quenching methodology generates crystalline phases within the glass phase, i.e. glass-ceramics.

4.3.2 Sol-gel methodology

The sol-gel methodology is based on the hydrolysis and condensation of the glass former precursors (e.g. silicon and aluminium alkoxides, etc.) solubilised in specific solvents (e.g. water, ethanol, etc.). It also involves the addition of nitrates or chlorides of the glass modifiers (e.g. calcium nitrate, etc.) to the processing solution and the use of specific catalytic and/or initiator conditions (e.g. ammonium hydroxide, etc.). This approach presents a series of

advantages compared to the melt-quenching approach, namely: a better compositional control; morphological control (e.g. particles, fibers, membranes, etc.); lower processing temperatures; among others [54].

The main reactions occurring during the sol-gel methodology are the hydrolysis of the glass precursors and their subsequent condensation. For the first step to occur it is essential the presence of an hydrolyzing medium (e.g. water) in order to produce the hydroxides/acids of the glass formers (e.g. silicic acid, aluminium hydroxide, etc.). The condensation reaction (second step) occurs between the different hydroxides/acids with the release of water molecules. This step is usually catalysed by different compounds, e.g. ammonium hydroxide, nitric acid, etc. [55]. Depending on the targeted morphology, the methodology can include an additional step usually designated as gelation. In this step the colloidal solution of particles is aged allowing their condensation into a macroscopic system (Figure 5) [14].

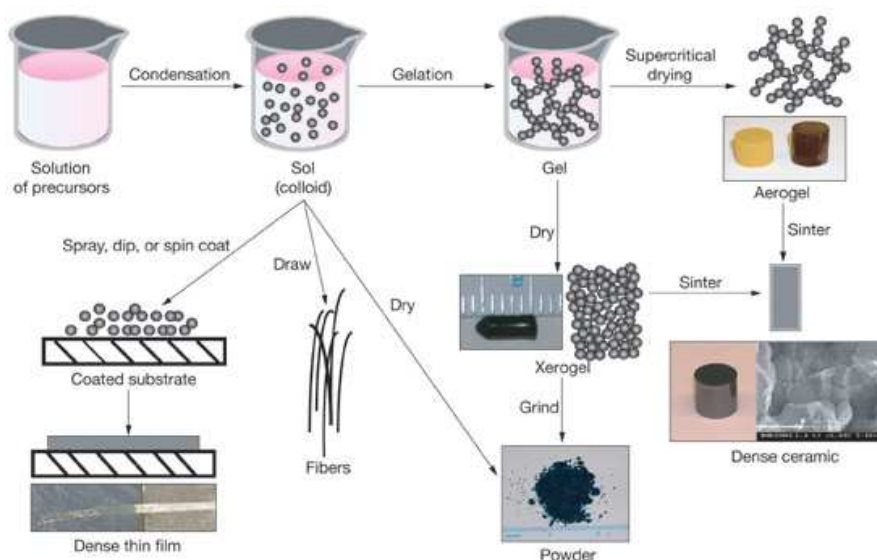


Figure 5: Sol-gel process (<https://www.llnl.gov/str/May05/Satcher.html>).

The whole sol-gel methodology is performed at lower temperatures than the melt-quenching approach. This characteristic imparts the valuable advantage of enabling the preparation of glasses incorporating bioactive compounds (e.g. proteins, drugs, etc.) sensitive to high temperatures [56, 57]. Moreover, glasses produced by this methodology usually present higher specific surface area and bioactivity [58].

4.4 The polymeric component

The GICs curing reactions only occurs if the polymeric component present significant acidity. Throughout the development and optimization of GIC different polymers have been tested in the formulations. As examples, can be pointed out PAA, poly (acrylic acid-co-itaconic acid) and poly (acrylic-co-maleic acid) with structural formulas presented in Figure 6 [59].

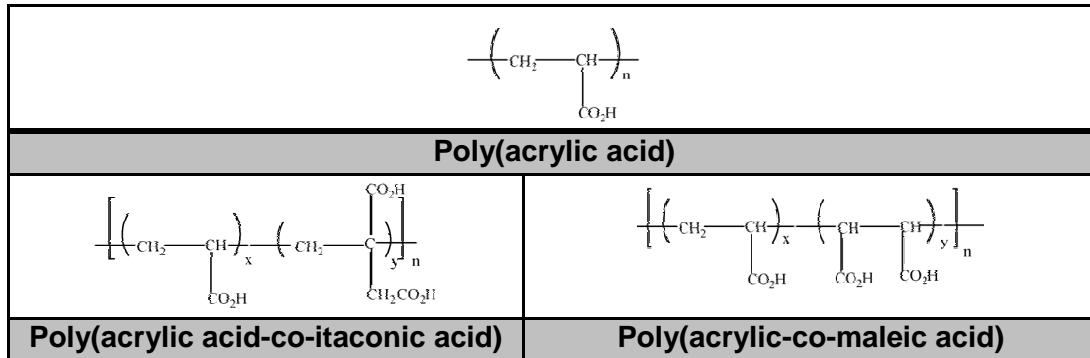


Figure 6: Polymers already tested in the development of GIC formulations.

From all the polymeric components tested until today PAA continues to be the most used in GIC formulations. This is essentially due to its high acidity, availability and lower price when compared to the other tested polymers [59]. The PAA molecular weight (M_w) directly influences cement mechanical behaviour and the cement paste initial viscosity. GIC mechanical performance is enhanced with PAA of high M_w , although, their high viscosity limits the homogeneity and mixability of the cement pastes. In this perspective, it is important to obtain a compromise between these two properties. The optimal formulations are prepared with polymeric components that have the highest M_w without significantly affecting the viscosity of the cement paste [60-63].

4.5 GIC curing reactions

GICs are formed when an acid-base reaction occurs between the glass powder and an aqueous solution of PAA, creating an inorganic-organic interlinked structure. The curing mechanism is composed by two general steps, gelation (Figure 7) and maturation.

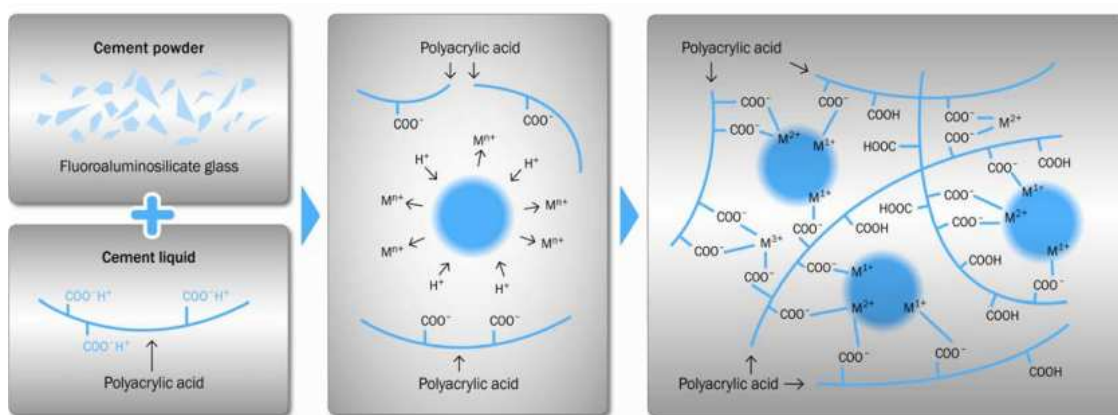


Figure 7: GICs curing reactions during the gelation stage [64].

During gelation, hydrated protons from the PAA/H₂O penetrate the surface of the glass particles and attack its basic sites (i.e. cations such as Na⁺, Ca²⁺, octahedral Al³⁺, etc.). The cations from the surface layer are leached to the cement matrix, promoting the ionic cross-linking of the PAA chains, through their carboxylate anions. This step usually occurs under a timeframe of approximately, 30 min. During the maturation step the tetrahedral aluminium present in the glass particle surface layer is leached under the same type of PAA acid attack. The longer timeframe of this maturation step (approximately, 24h) is attributed to the higher stability of the tetrahedral aluminium that is covalently bounded within the glass structure [34, 41, 50, 65-70].

4.6 Properties, applications and importance of GICs and its constituents

4.6.1 Properties of GICs

There are a series of advantages on using GIC as cementation agent of different dental restorations, namely: chemical adhesion to tooth; anti-cariogenic effect; mechanical behaviour under compression loading; among others. The GIC chemical adhesion to the tooth is due to the dentin chemical structure. This is one of the main advantages of the GICs and is based on formation of ionic cross-links between the PAA carboxylate anions and the Ca²⁺ from the dentin's hydroxyapatite [71]. Their anti-cariogenic effect is mainly related with the use of fluorine in the glass compositions. Fluorine is gradually leached from GIC to the

surrounding dentin strengthening the tooth resistance to bacterial proliferation [44, 72]. Moreover, it has been proven that GICs are able to act as a fluorine reservoir. In this sense GICs are not only leaching fluorine to the surrounding tissue but is also able to uptake additional fluorine from the surroundings (e.g. toothpastes) [73]. In relation to the mechanical behaviour, Kenny *et al* reported that it depends on the molecular weight (M_w) of PAA [74]. Additionally, the powder to liquid ratio [75], concentration of PAA and the use of chelating agents also influences the final performance of the GICs. In general, the available formulations achieve compressive strengths up to 200 MPa and biaxial flexural strengths up to 50 MPa. The ratio of “bound” and “unbounded” water is a determinant factor affecting the GIC properties. In fact, the highest is the proportion of “unbounded” water the lower is the mechanical performance and the GIC general stability. Finally, the glass particle size also influences significantly the mechanical behaviour of the GICs and the cement curing reactions. The lower the glass particle size, the higher is its surface area and lower is the GIC crack deflection [76]. The main drawback of the reduction of the particle size is related with the faster setting kinetics. This variation reduces the time available to the medical doctor to manipulate the cement paste and to apply it at the intervention site. In this sense, it is always desirable to obtain a compromise between glass particle size, mechanical properties and GIC setting kinetics to develop optimized formulations.

A number of modifications can be made in the formulations to enhance the GIC properties, namely: (1) alternative polymers, as the polyacid component; (2) dried polymers blended with the glass and activation by the addition of water; (3) ceramic-metal hybrid cements; (4) metal-reinforced cement for enhanced mechanical properties; (5) resin-modified GICs (RMGICs) using initiators and resins capable of undergoing photochemical polymerization [35, 77].

GICs have demonstrated to possess biocompatibility and bioactivity. These cements are able to release osteoconductive ions such as calcium and fluoride to the surrounding tissue [65]. The incorporation of strontium in the glass formulations has been done for several years due to its characteristic properties, namely: radiopacifier, antibacterial properties and can help in the regeneration of healthy bone. In fact, it has been proven that low doses of

strontium ($300 \text{ mg Kg}^{-1} \text{ day}^{-1}$ of Sr^{2+} for 9 weeks) can stimulate bone formation and inhibit bone resorption in both animal and humans. Strontium has an affinity for bone being incorporated by surface exchange and ionic substitution [78].

4.6.2 Applications of GICs

GICs have been tested in the cementation of different biomaterials dedicated to the repair or substitution of tooth and bone. Its main application area continues to be the dentistry field, where conventional GICs are used to cement different types of composites used to repair teeth or as temporary filler before the application of a definitive dental restoration. Non-conventional GICs, such as the RMGICs have been additionally proposed as definitive dental restorations [44, 79-81].

Hurrell-Gillingham and co-workers suggest that the main properties of GICs (including adhesion to mineralized tissues, minimal exotherm during setting and good biocompatibility) enables them to be exploited in the otology field [82]. Although, the most relevant and underexploited application of GIC remains to be in the orthopaedic field as bone cements [74].

4.6.3 Biocompatibility of GICs

GICs are not bioinert but should be classified as bioactive. Hatton and co-workers tested a set of GICs under *in vitro* cell culture and they demonstrated that some GICs are biocompatibility. Although, other studies proved that the ions present in GICs namely aluminium and fluoride are responsible for the toxicity of some formulations. These studies also report a relation between the toxicity of the formulations and the ionic concentrations and culture conditions [83].

4.6.4 The importance of GIC cations in the regeneration of tissue

The GICs have been tested *in vivo* with encouraging results. The formation of bone was observed in some formulations after 6 weeks of implantation and being stable during 1 year. In addition, in the short term there is an inflammatory response observed in soft tissues adjacent to the GIC. The tissue reaction was caused by one or both of the following factors:

(i) Reduction of tissue pH due to the acidic PAA. This is the most probable cause of tissue necrosis (a damage of the surrounding tissues).

(ii) Release of free glass particles from the cement to the surrounding tissues. This is probably induced by the excess of water originated on the surrounding tissue that migrates to the GIC affecting its curing reactions and promoting the release of glass particles. Glass particles are known to cause inflammatory response in adjacent soft tissues. In surgery (e.g. dentistry), it is important to avoid excess of the moisture contamination during placement of the GICs.

A limited dose of ion release is the significant factor that determines tissue response to regeneration. In contrast, as previously mentioned, high levels of ionic leaching from the GIC can produce inflammatory response. Upon GIC application it is expectable an initial time period where inflammation occurs in the surrounding tissue due to higher levels of ionic and PAA leaching from the GIC. After this initial timeframe the inflammatory response is suppressed and the GIC appears with a layer of relatively mature bone tissue. At this stage the osteoconductive potential of the GIC is evident (a property not common in other types of bone cements) [83].

a) Aluminium and its toxicity

Aluminium in the ionic form (Al^{3+}) has several implications in human health and its toxicity has been studied by several authors. This cation is responsible for many degenerative diseases including Alzheimer's and Parkinson's. Boyce and co-workers reported that encephalopathy and osteomalacia was detected in patients being subject to dialysis. It was observed that the water used in the dialysis contained high levels of aluminium. Bone biopsies detected the presence of high levels of aluminium in the bone, confirming that the origin of the detected pathologies was the aluminium present in the water used for the dialysis [84].

Another case study (a bone reconstruction of a woman with 52 years old) was reported by *Reusche et al.* This reconstruction was performed with a GIC prepared by mixing a calcium aluminium fluorosilicate glass and an aqueous solution of polycarboxylic acid. This GIC (Ionocem) contained high levels of

aluminium and six weeks after implantation the patient presented a fatal aluminium encephalopathy (see Figure 8) [85].

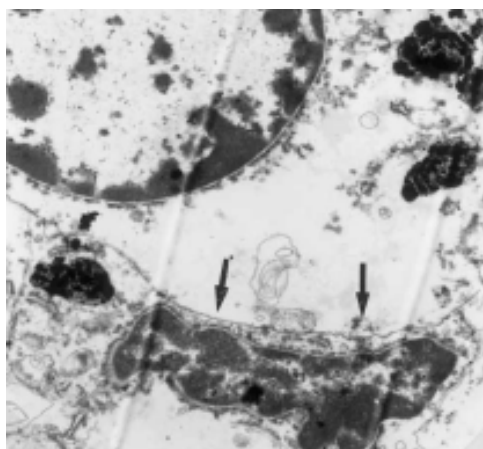


Figure 8: Aluminium inflammatory response of Al-based GICs resulting in an irregular density at the specific positions (arrowheads) [85].

In general, it has been accepted that the release of aluminium present in the GICs formulations, used as bone cements, produces a deleterious effect in the health of the intervened patients [85]. Although, this has been considered a critical component of the glass compositions used to prepare GICs. In fact, it has been proposed that Al^{3+} has a critical role in the formation of the PAA carboxylate cross-links within the GIC cement matrix [86]. Under this perspective, Boyd and co-workers tested several aluminium-free glass compositions and their cement forming ability. Under these studies the same authors found that glass compositions where aluminium was substituted by zinc are able to produce GIC. The developed formulations presented properties that are consistent with their application in orthopaedic procedures, according to ISO5833 [78, 87].

b) Other relevant cations

There are a series of other cations that possess a relevant role in the setting chemistry and final properties of the GICs. As stated before, zinc has demonstrated that it is able to substitute aluminium in the glass compositions used to prepare GICs. Although not completely proven, it is reported that zinc imparted other relevant properties to the final GICs, namely: bactericidal and bioactivity. Zinc is also an essential trace element which presents effects on *in*

vitro and *in vivo* bone formation and bone protein synthesis. It promotes the proliferation of osteoblasts and many biological functions. It promotes new bone formation in the surroundings of the implants [88]. Additionally, zinc deficiency may be a risk factor in the pathogenesis of osteoporosis [89].

Their bivalency makes the cations derived from the elements of the second group of the periodic table, namely, magnesium, calcium and strontium, suitable to act as PAA ionic cross-linkers. In fact, calcium has been described as the second most relevant cations in the GIC setting chemistry [90]. It has been reported in the glass composition since the initial development of the GICs. Its role is similar to aluminium in the cross-linking of the PAA network through calcium-carboxylate ionic linkages. Due to their similar characteristic, magnesium and strontium have an equivalent potential. In contrast, beryllium and barium are usually not included due to their toxicity.

The nature of strontium and its biological function has not been investigated as extensively as the role of calcium and magnesium of the same chemical family. Strontium is believed to have a participation in dental tissue mineralization due to their properties similar to those presented by calcium. Its antibacterial effect has been claimed but remains to be clarified: previous *in vitro* work on commercial RMGIC (Fuji II LC) showed that strontium was not cytotoxic when in contact with human osteoblastic cells. Strontium, as a substitute of calcium in hydroxyapatite, has been studied recently and claimed to prevent bone fractures [90]. In addition, strontium may inhibit osteoclastic turnover and promote the osteoblastic one. Moreover, bone strength increases and the risk of fractures decrease [91, 92]. It has been also reported to contribute to the increase in bone mass and volume when given at low doses, re-mineralizing skeletal lesions. It seems that strontium directly suppresses bone resorption and has no deleterious effect on bone mineralization. Strontium has also reported to have beneficial effects on bone formation in rodents and humans which results in increased trabecular volume. It has been also confirmed that strontium increases the bone strength and in bone density due to its higher atomic weight in comparison with calcium. Strontium is currently used as dopant of the crystalline structures of calcium salts to improve their biological properties. The successful incorporation of strontium ions in the composition of

hydroxyapatite, calcium phosphate cements and calcium silicates help on the proliferation and activity of osteoblastic cells [58]. Finally, Johnson *et al.* studied the effect of the incorporation of strontium in GICs. They reported a relation between the presence of strontium in the GIC and a marked reduction of bone ash; increase in the amount of magnesium and potassium in the bone; and by depressed calcium contents as compared to normal bone [93].

Drouet *et al.* studied the effect of strontium and magnesium in the formation of apatites. They observed that the magnesium taken up was found to be reversibly fixed to the apatite structure independently of their maturation stage. In contrast, the amount of reversibly fixed strontium decreased noticeably with maturation in a strontium-containing solution. These findings suggested that magnesium remained mostly on the surface of nanocrystalline apatites whereas strontium was progressively incorporated into the growing apatite domains [94].

Magnesium is a cation that presents high physiological interests in the biomedical field. It is essential to human metabolism and is naturally present in the bone. It may actually have stimulatory effects on the growth of new bone and it is classified as an essential element for the human body [88].

Bibliography

1. An, Y.H. and R.A. Draughn, eds. *Mechanical Testing of Bone and the Bone–Implant Interface*. 2000, CRC Press: Boca Raton.
2. Beniash, E., *Biomaterials—hierarchical nanocomposites: the example of bone*. Wiley Interdisciplinary Reviews: Nanomedicine and Nanobiotechnology, 2011. **3**(1): p. 47-69.
3. Biltz, R.M. and E.D. Pellegrino, *The Chemical Anatomy of Bone: I. A comparative study of bone composition in sixteen vertebrates*. J Bone Joint Surg Am, 1969. **51**(3): p. 456-466.
4. Da Cruz GA, d.T.S., Sallum EA, de Lima AF, *Morphological and chemical analysis of bone substitutes by scanning electron microscopy and microanalysis by spectroscopy of dispersion energy*. Braz Dent J., 2007. **18**(2): p. 129-33.
5. Tzaphlidou, M., *The role of collagen in bone structure: An image processing approach*. Micron. **36**(7-8): p. 593-601.
6. Rho, J.-Y., L. Kuhn-Spearing, and P. Zioupos, *Mechanical properties and the hierarchical structure of bone*. Medical engineering & physics, 1998. **20**(2): p. 92-102.
7. Hadjidakis, D.J. and I.I. Androulakis, *Bone Remodeling*. Annals of the New York Academy of Sciences, 2006. **1092**(1): p. 385-396.
8. Reis, R.L.a.S.R., J., *Biodegradable Systems in Tissue Engineering and Regenerative Medicine*. CRC Press. 2005.
9. Gupta, H.S. and P. Zioupos, *Fracture of bone tissue: The 'hows' and the 'whys'*. Medical engineering & physics, 2008. **30**(10): p. 1209-1226.
10. Hench, L.L., Jones J. R., *Biomaterials, artificial organs and tissue engineering*. 2005.
11. Reichert, W.M., *Indwelling Neural Implants: Strategies for Contending with the In Vivo Environment*. 2008.
12. Aubin, J.E., *Bone Stem Cells*. Journal of Cellular Biochemistry Supplements, 1998. **30**(31): p. 73–82.
13. Park, J.B., *Biomaterials: Principles and Applications*. 2002.
14. Abou Neel, E.A., et al., *Bioactive functional materials: a perspective on phosphate-based glasses*. Journal of Materials Chemistry, 2009. **19**(6): p. 690-701.
15. Hench, L.L., et al., *Glass and Medicine*. International Journal of Applied Glass Science, 2010. **1**(1): p. 104-117.
16. Navarro, M., et al., *Biomaterials in orthopaedics*. Journal of the Royal Society Interface, 2008. **5**(27): p. 1137-1158.
17. Ginebra, M.P., et al., *New processing approaches in calcium phosphate cements and their applications in regenerative medicine*. Acta Biomaterialia, 2010. **6**(8): p. 2863-2873.

18. Ducheyne, P., *Bioactive ceramics*. J Bone Joint Surg Br, 1994. **76-B**(6): p. 861-862.
19. Gulotta, L.V., et al., *Augmentation of Tendon-to-Bone Healing With a Magnesium-Based Bone Adhesive*. The American Journal of Sports Medicine, 2008. **36**(7): p. 1290-1297.
20. Barbucci, R., ed. *Integrated Biomaterials Science*. 2002, Kluwer Academic Publishers: New York.
21. Barrios de Arenas, I., C. Schattner, and M. Vásquez, *Bioactivity and mechanical properties of Na₂O·CaO·SiO₂·P₂O₅ modified glasses*. Ceramics International, 2006. **32**(5): p. 515-520.
22. Bellucci, D., et al., *Potassium based bioactive glass for bone tissue engineering*. Ceramics International, 2010. **36**(8): p. 2449-2453.
23. Moshaverinia, A., et al., *Effects of incorporation of hydroxyapatite and fluoroapatite nanobioceramics into conventional glass ionomer cements (GIC)*. Acta Biomaterialia, 2008. **4**(2): p. 432-440.
24. Chevalier, J. and L. Gremillard, *Ceramics for medical applications: A picture for the next 20 years*. Journal of the European Ceramic Society, 2009. **29**(7): p. 1245-1255.
25. Sastre, R., de Aza, S., San Román, J., *Ingeniería de Tejidos: Principios Básicos, Soportes y Células Madre, In Biomaterials*, F.E.I. S.L, Editor. 2004.
26. Coleman, N.J., K. Awosanya, and J.W. Nicholson, *Aspects of the in vitro bioactivity of hydraulic calcium (aluminosilicate) cement*. Journal of Biomedical Materials Research Part A, 2009. **90A**(1): p. 166-174.
27. Brink, M., et al., *Compositional dependence of bioactivity of glasses in the system Na₂O-K₂O-MgO-CaO-B₂O₃-P₂O₅-SiO₂*. Journal of Biomedical Materials Research, 1997. **37**(1): p. 114-121.
28. Hee-Gon Bang, S.-J.K.a.S.-Y.P., *Biocompatibility and the physical properties of bio-glass ceramics in the Na₂O-CaO-SiO₂-P₂O₅ system with CaF₂ and MgF₂ additives*. Journal of Ceramic Processing Research, 2008. **9**(6): p. 588-590.
29. Gomes, M.E. and R.L. Reis, *Biodegradable polymers and composites in biomedical applications: from catgut to tissue engineering. Part 1 Available systems and their properties*. International Materials Reviews, 2004. **49**(5): p. 261-273.
30. Gomes, M.E. and R.L. Reis, *Biodegradable polymers and composites in biomedical applications: from catgut to tissue engineering. Part 2 Systems for temporary replacement and advanced tissue regeneration*. International Materials Reviews, 2004. **49**(5): p. 274-285.
31. Boesel, L. and R. Reis, *Hydrophilic matrices to be used as bioactive and degradable bone cements*. Journal of Materials Science: Materials in Medicine, 2004. **15**(4): p. 503-506.
32. Silva, G.A., et al., *The effect of starch and starch-bioactive glass composite microparticles on the adhesion and expression of the*

- osteoblastic phenotype of a bone cell line*. Biomaterials, 2007. **28**(2): p. 326-334.
33. Tester, R.F., J. Karkalas, and X. Qi, *Starch—composition, fine structure and architecture*. Journal of Cereal Science, 2004. **39**(2): p. 151-165.
 34. Wilson, A.D. and B.E. Kent, *Glass-Ionomer Cement, a New Translucent Dental Filling Material*. Journal of Applied Chemistry and Biotechnology, 1971. **21**(11): p. 313-&.
 35. Nicholson, J.W., *Chemistry of glass-ionomer cements: a review*. Biomaterials, 1998. **19**(6): p. 485-494.
 36. De Barra, E. and R.G. Hill, *Influence of glass composition on the properties of glass polyalkenoate cements. Part III: influence of fluorite content*. Biomaterials, 2000. **21**(6): p. 563-569.
 37. Guida, A., et al., *Fluoride release from model glass ionomer cements*. Journal of Materials Science: Materials in Medicine, 2002. **13**(7): p. 645-649.
 38. Yap, A.U.J., et al., *Experimental studies on a new bioactive material: HA-Ionomer cements*. Biomaterials, 2002. **23**(3): p. 955-962.
 39. Álvaro DELLA BONA, C.P., Vinícius ROSA, *EFFECT OF ACID ETCHING OF GLASS IONOMER CEMENT SURFACE ON THE MICROLEAKAGE OF SANDWICH RESTORATIONS*. J Appl Oral Sci., 2007. **15**(3): p. 230-234.
 40. Bertolini, M.J., M.A. Zaghete, and R. Gimenes, *Development of an experimental glass ionomer cement containing niobium and fluoride*. Journal of Non-Crystalline Solids, 2005. **351**(52-54): p. 3884-3887.
 41. Bertolini, M.J., et al., *Determination of the properties of an experimental glass polyalkenoate cement prepared from niobium silicate powder containing fluoride*. Dental Materials, 2008. **24**(1): p. 124-128.
 42. Bresciani E, B.T., Fagundes T C, Adachi A, Terrin M M, Navarro M F, *Compressive and diametral tensile strength of glass ionomer cements*. Journal Of Minimum Intervention In Dentistry, 2008. **1**(2): p. 102-111.
 43. Crisp S, L.B., Wilson AD, *Glass ionomer cements: chemistry of erosion*. J Dent Res., 1976. **55**(6): p. 1032-1041.
 44. Guida A, H.R., Towler MR, Eramo S., *Fluoride release from model glass ionomer cements*. J Mater Sci Mater Med. 2002 Jul;13(7):645-9., 2002. **13**(7): p. 645-649.
 45. Lohbauer, U., et al., *Reactive fibre reinforced glass ionomer cements*. Biomaterials, 2003. **24**(17): p. 2901-2907.
 46. Gu, Y.W. and Y.Q. Fu, *Heat treatment and thermally induced crystallization of glass for glass ionomer cement*. Thermochimica Acta, 2004. **423**(1-2): p. 107-112.
 47. Pires, R.A., C. Fernandez, and T.G. Nunes, *Structural and spatially resolved studies on the hardening of a commercial resin-modified glass-ionomer cement*. Journal of Materials Science-Materials in Medicine, 2007. **18**(5): p. 787-796.

48. THOMAS I. BARRY, D.J.C.a.A.D.W., *The Structure of a Glass-Ionomer Cement and its Relationship to the Setting Process*. J DENT RES, 1979. **58**(3): p. 1072-1079.
49. Zainuddin, N., et al., *A long-term study on the setting reaction of glass ionomer cements by ^{27}Al MAS-NMR spectroscopy*. Dental Materials, 2009. **25**(3): p. 290-295.
50. Oliva, A., et al., *Biocompatibility studies on glass ionomer cements by primary cultures of human osteoblasts*. Biomaterials, 1996. **17**(13): p. 1351-1356.
51. Nakajima, H., H. Komatsu, and T. Okabe, *Aluminum ions in analysis of released fluoride from glass ionomers*. Journal of Dentistry, 1997. **25**(2): p. 137-144.
52. Brook, I.M. and P.V. Hatton, *Glass-ionomers: bioactive implant materials*. Biomaterials, 1998. **19**(6): p. 565-571.
53. Kawano, F., et al., *Reinforcement effect of short glass fibers with $\text{CaO-P}_2\text{O}_5\text{-SiO}_2\text{-Al}_2\text{O}_3$ glass on strength of glass-ionomer cement*. Journal of Dentistry, 2001. **29**(5): p. 377-380.
54. Hench, L.L. and J.K. West, *The sol-gel process*. Chemical Reviews, 1990. **90**(1): p. 33-72.
55. Wren, A., et al., *The effect of glass synthesis route on mechanical and physical properties of resultant glass ionomer cements*. Journal of Materials Science: Materials in Medicine, 2009. **20**(10): p. 1991-1999.
56. Brunner, T.J., R.N. Grass, and W.J. Stark, *Glass and bioglass nanopowders by flame synthesis*. Chemical Communications, 2006(13): p. 1384-1386.
57. Cestari, A., et al., *Characterization of the calcium-fluoroaluminosilicate glass prepared by a non-hydrolytic sol-gel route for future dental application as glass ionomer cement*. Materials Research, 2009. **12**: p. 139-143.
58. Hesarak, S., et al., *The effect of Sr concentration on bioactivity and biocompatibility of sol-gel derived glasses based on $\text{CaO-SrO-SiO}_2\text{-P}_2\text{O}_5$ quaternary system*. Materials Science and Engineering: C, 2010. **30**(3): p. 383-390.
59. Culbertson, B.M., *New polymeric materials for use in glass-ionomer cements*. Journal of Dentistry, 2006. **34**(8): p. 556-565.
60. Hill, R.G., A.D. Wilson, and C.P. Warrens, *The influence of poly(acrylic acid) molecular weight on the fracture toughness of glass-ionomer cements*. Journal of Materials Science, 1989. **24**(1): p. 363-371.
61. Fennell, B. and R.G. Hill, *The influence of poly(acrylic acid) molar mass and concentration on the properties of polyalkenoate cements Part I Compressive strength*. Journal of Materials Science, 2001. **36**(21): p. 5193-5202.
62. Fennell, B. and R.G. Hill, *The influence of poly(acrylic acid) molar mass and concentration on the properties of polyalkenoate cements Part II*

- Young's modulus and flexural strength*. Journal of Materials Science, 2001. **36**(21): p. 5177-5183.
63. Kenny, S.M. and M. Buggy, *Bone cements and fillers: A review*. Journal of Materials Science: Materials in Medicine, 2003. **14**(11): p. 923-938.
 64. Lohbauer, U., *Dental Glass Ionomer Cements as Permanent Filling Materials? – Properties, Limitations and Future Trends*. Materials, 2009. **3**(1): p. 76-96.
 65. Blades, M.C., et al., *In vivo skeletal response and biomechanical assessment of two novel polyalkenoate cements following femoral implantation in the female New Zealand White rabbit*. Journal of Materials Science: Materials in Medicine, 1998. **9**(12): p. 701-706.
 66. Kajiwarra, M., *Formation and compressive strength of the ionomer cements prepared from aluminosilicate glass and poly(acrylic acid)*. Journal of Materials Science Letters, 1984. **3**(7): p. 617-619.
 67. Kamitakahara, M., et al., *Effect of polyacrylic acid on the apatite formation of a bioactive ceramic in a simulated body fluid: fundamental examination of the possibility of obtaining bioactive glass-ionomer cements for orthopaedic use*. Biomaterials, 2001. **22**(23): p. 3191-3196.
 68. Limapornvanich, A., et al., *Bovine serum albumin release from novel chitosan-fluoro-aluminosilicate glass ionomer cement: Stability and cytotoxicity studies*. Journal of Dentistry, 2009. **37**(9): p. 686-690.
 69. Gu, Y.W., et al., *Development of zirconia-glass ionomer cement composites*. Journal of Non-Crystalline Solids, 2005. **351**(6-7): p. 508-514.
 70. Khalil, S.K.H. and E.D.T. Atkins, *Investigation of glass–ionomer cements using differential scanning calorimetry*. Journal of Materials Science: Materials in Medicine, 1998. **9**(9): p. 529-533.
 71. Boesel, L.F., et al., *The in vitro bioactivity of two novel hydrophilic, partially degradable bone cements*. Acta Biomaterialia, 2007. **3**(2): p. 175-182.
 72. Griffin, S.G. and R.G. Hill, *Influence of glass composition on the properties of glass polyalkenoate cements. Part IV: influence of fluorine content*. Biomaterials, 2000. **21**(7): p. 693-698.
 73. Brauer, D.S., et al., *Fluoride-containing bioactive glasses: Effect of glass design and structure on degradation, pH and apatite formation in simulated body fluid*. Acta Biomaterialia, 2010. **6**(8): p. 3275-3282.
 74. Kenny, S., R.G. Hill, and M. Towler, *The influence of poly(acrylic acid) molar mass on the properties of polyalkenoate cements formed from zinc oxide/apatite mixtures*. Journal of Materials Science: Materials in Medicine, 2000. **11**(12): p. 847-853.
 75. Aratani, M., et al., *Compressive strength of resin-modified glass ionomer restorative material: effect of P/L ratio and storage time*. Journal of Applied Oral Science, 2005. **13**: p. 356-359.

76. Brandt, B., et al., *The Influence of Particle Size on the Mechanical Properties of Dental Glass Ionomer Cements*. Advanced Engineering Materials, 2010. **12**(12): p. B684-B689.
77. Boesel, L.F., M.H.V. Fernandes, and R.L. Reis, *The behavior of novel hydrophilic composite bone cements in simulated body fluids*. Journal of Biomedical Materials Research Part B: Applied Biomaterials, 2004. **70B**(2): p. 368-377.
78. Boyd, D., et al., *Zinc-based glass polyalkenoate cements with improved setting times and mechanical properties*. Acta Biomaterialia, 2008. **4**(2): p. 425-431.
79. Fathi, H., et al., *The effect of calcium fluoride (CaF₂) on the chemical solubility of an apatite-mullite glass-ceramic material*. Dental Materials, 2005. **21**(6): p. 551-556.
80. Berg, J.H., *Glass ionomer cements*. Pediatric Dentistry, 2002. **24**(5): p. 430-438.
81. De Bruyne, M.A.A. and R.J.G. De Moor, *The use of glass ionomer cements in both conventional and surgical endodontics*. International Endodontic Journal, 2004. **37**(2): p. 91-104.
82. Hurrell-Gillingham, K., et al., *Devitrification of ionomer glass and its effect on the in vitro biocompatibility of glass-ionomer cements*. Biomaterials, 2003. **24**(18): p. 3153-3160.
83. Hatton, P.V., K. Hurrell-Gillingham, and I.M. Brook, *Biocompatibility of glass-ionomer bone cements*. Journal of Dentistry, 2006. **34**(8): p. 598-601.
84. Boyce, *Toxic effect of aluminium and others substances on bone turnover*.
85. Reusche, E., et al., *Subacute fatal aluminum encephalopathy after reconstructive otoneurosurgery: A case report*. Human Pathology, 2001. **32**(10): p. 1136-1140.
86. Boyd, D. and M. Towler, *The processing, mechanical properties and bioactivity of zinc based glass ionomer cements*. Journal of Materials Science: Materials in Medicine, 2005. **16**(9): p. 843-850.
87. Boyd, D., et al., *The antibacterial effects of zinc ion migration from zinc-based glass polyalkenoate cements*. Journal of Materials Science: Materials in Medicine, 2006. **17**(6): p. 489-494.
88. Dietrich, E., et al., *Effects of Mg and Zn on the surface of doped melt-derived glass for biomaterials applications*. Applied Surface Science, 2008. **255**(2): p. 391-395.
89. Johal, K.K., et al., *In vivo response of strontium and zinc-based ionomeric cement implants in bone*. Journal of Materials Science: Materials in Medicine, 2002. **13**(4): p. 375-379.
90. Dabsie, F., et al., *Does strontium play a role in the cariostatic activity of glass ionomer?: Strontium diffusion and antibacterial activity*. Journal of Dentistry, 2009. **37**(7): p. 554-559.

91. Boyd, D., et al., *TEM analysis of apatite surface layers observed on zinc based glass polyalkenoate cements*. Journal of Materials Science, 2008. **43**(3): p. 1170-1173.
92. Bazin, D., et al., *Revisiting the localisation of Zn²⁺ cations sorbed on pathological apatite calcifications made through X-ray absorption spectroscopy*. Biochimie, 2009. **91**(10): p. 1294-1300.
93. Johnson, A., *The influence of strontium on characteristic factors of bone*. Calcified Tissue International, 1973. **11**(3): p. 215-221.
94. Drouet, C., et al., *Surface enrichment of biomimetic apatites with biologically-active ions Mg²⁺ and Sr²⁺: A preamble to the activation of bone repair materials*. Materials Science and Engineering: C, 2008. **28**(8): p. 1544-1550.

Chapter II






Materials and Methods

This chapter compiles the information relative to the materials used during the experimental procedures, and the methodologies employed in the synthesis and characterization of the developed GICs.

1. Materials

The safety information, purity and supplier of the chemicals used for the glass synthesis and in the formulation of the cements are presented in Table 1. Each reagent was used at specific proportions to prepare glasses of different compositions. The addition of corn starch to the cement formulation was tested in an attempt to improve its biodegradability. α -Amylase was used as a degradation catalyser in the starch-containing formulations.

Table 1: Specifications of all reagents used for the glass and cement preparation.

Reagent	Supplier	Purity	Hazard Codes	Symbol
Sodium Hydrogen carbonate (NaHCO_3)	Riedel de-Haen	99.70 %	Not Hazardous	-
Calcium carbonate (CaCO_3)	Sigma	99 %	Xi	
Magnesium oxide (MgO)	Sigma	98 %	ND	-
Diammonium hydrogen phosphate ($(\text{NH}_4)_2\text{HPO}_4$)	Sigma	98.00 %	Xi	
Zinc oxide (ZnO)	Sigma	nd	ND	-
Strontium carbonate (SrCO_3)	Sigma	98 %	ND	-
Silica (SiO_2)	Merck	nd	T	
Polyacrylic acid ($\text{Mw}=50\text{kDa}$)	Sigma	nd	ND	-
Polyacrylic acid ($\text{Mw}=450\text{kDa}$)	Sigma	nd	T	
Polyacrylic acid ($\text{Mw}=1250\text{kDa}$)	Sigma	nd	ND	-
Corn starch	Sigma	nd	Not Hazardous	-
α -amylase	Sigma	nd	Xn	

2. Materials synthesis and processing

2.1 Glass synthesis

Glass formulations were prepared by mixing the appropriate quantities of the glass precursors in a mortar using ethanol as a mixing adjuvant. The final glass compositions are detailed in Table 2.

Table 2: Composition of the synthesized glass formulations.

Component	G1*	G2	G3	G4	G5	G6
SiO ₂ (SiO ₂)	0.340	0.340	0.340	0.340	0.340	0.340
ZnO (ZnO)	0.300	0.300	0.300	0.300	0.300	0.300
MgO (MgO)	0.250	-	-	0.125	-	0.125
CaO (CaCO ₃)	-	0.250	-	0.125	0.125	-
SrO (SrCO ₃)	-	-	0.250	-	0.125	0.125
Na ₂ O (NaHCO ₃)	0.050	0.050	0.050	0.050	0.050	0.050
P ₂ O ₅ ((NH ₄) ₂ HPO ₄)	0.060	0.060	0.060	0.060	0.060	0.060

* Glass composition G1 did not melt at the experimental conditions used under this work. In this perspective G1 composition was not used to prepare GICs.

Upon mixing, the formulations were dried overnight in a vacuum oven at 35 °C [1-3]. The dried formulations were heated in a crucible to 300 °C for 30 minutes to release the ammonia from the diammonium hydrogen phosphate; 650 °C for 30 minutes to allow the release of carbon dioxide from the carbonates; and 1300 °C to allow the complete melting of the mixture [4, 5]. The melted mixtures were splat quenched by pouring the melt onto a metal plate maintained at room temperature (Figure 1) [6-13].

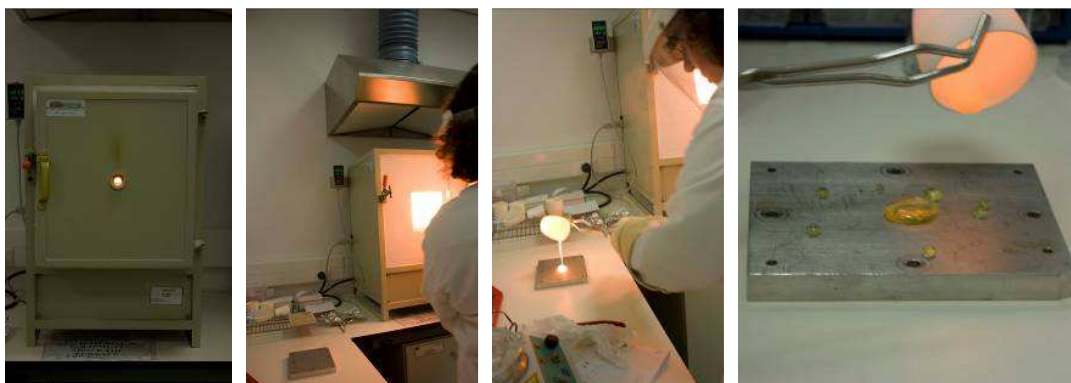


Figure 1: Illustration the melt quenching process.

The glass blocks were frozen with liquid nitrogen and grounded with a pestle and mortar (Figure 2). Upon size reduction the glass particles were separated by sizes using an Analytical Sieve Shaker (Retsch AS200) for 5 min at a rate of 60 rpm. With this methodology it was possible to collect the glass fractions that presented particle sizes of $x < 63 \mu\text{m}$, $63 \mu\text{m} < x < 125 \mu\text{m}$ and $125 \mu\text{m} < x < 250 \mu\text{m}$.



Figure 2: Glass powder preparation and sieving.

2.2 Cement preparation

Cement formulations were prepared by mixing the glass powder with PAA and water at appropriate amounts (55: 21: 24 by mass). After mixing, the cement pastes were introduced into a Teflon mould to produce cylindrical cement specimens of 6 mm diameter and 11 mm height (Figure 3).

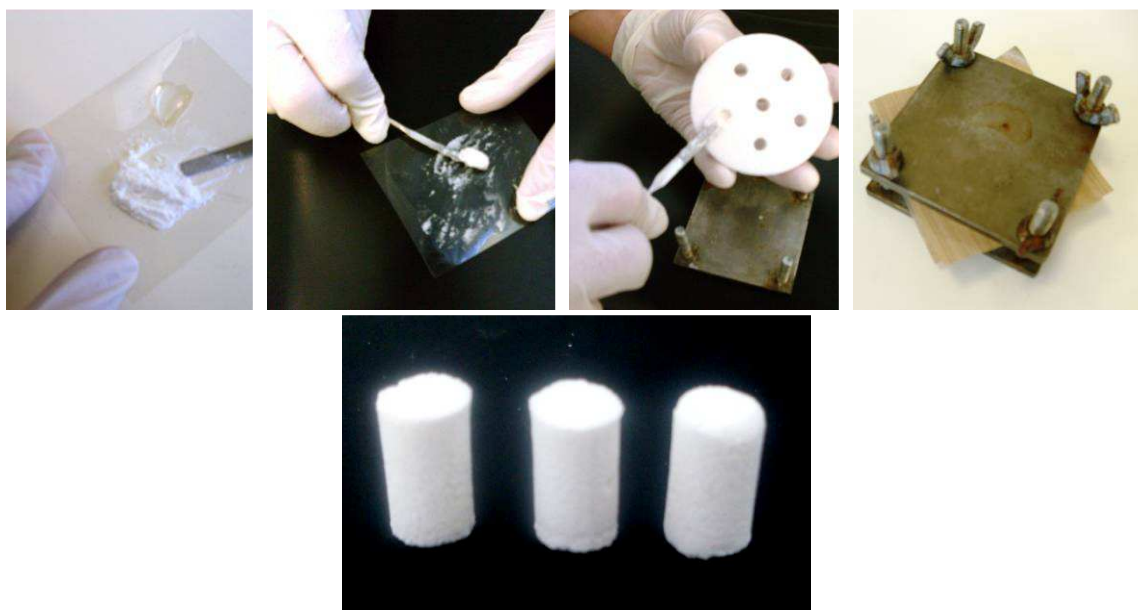


Figure 3: Example of the preparation of a moulded cement formulation.

The cement formulation that presented higher mechanical resistance was modified in an attempt to enhance its biodegradability. For this purpose it was added corn starch to the formulation (5 and 25 % by weight) [14].

3. Characterization methodologies

3.1 Mechanical performance under compression loading

All the developed cements were mechanically evaluated under compression loading. For each formulation it was prepared six cylindrical specimens (as detailed in the cement preparation section). The mechanical loading was executed on an Instron 5540 (Instron, USA) equipped with a load cell of 1 kN and 2 mm/min of crosshead speed (Figure 4). In all cases, the samples were maintained at room temperature for 24 hours prior to the mechanical testing [15].

From the stress-strain curves it was determined the compression modulus (CM) and the compressive strength (CS). The compression modulus was determined as the initial slope (elastic regime) of the stress-strain curves.

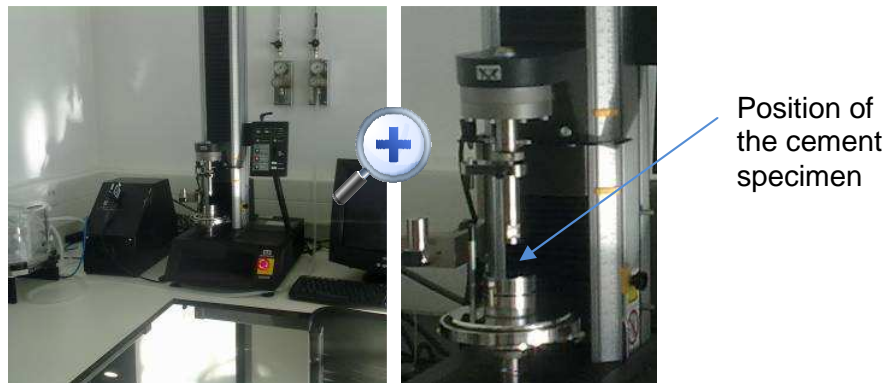


Figure 4: Instron 5540, Universal mechanical testing machine.

The CS was calculated from equation 1:

$$CS = \frac{4p}{\pi d^2}$$

Equation 1

where, CS is the compressive strength (MPa), ρ is the maximum applied load (N) and d is the diameter of the sample (mm) [11, 16, 17].

3.2 Fourier Transform Infrared spectroscopy

The evolution of the acid-base reaction between the glass particles and the PAA was followed by Fourier Transform Infrared (FTIR) spectroscopy. The FTIR spectra were acquired on KBr pellets. For this purpose, 400 mg of KBr (Sigma-Aldrich, >99 % trace metals basis) was mixed with 2-4 mg of sample in a mortar and pestle until forming an homogeneous mixture (Figure 5). This mixture was moulded to a pellet using a press (Pike, USA). The FTIR spectra were acquired on a Shimadzu IR-Prestige 21 spectrometer, under transmittance mode using a resolution of 4 cm^{-1} , a range between $4400\text{--}400\text{ cm}^{-1}$ and 32 scans.



Figure 5: Preparation of the KBr pellets.

3.3 X-ray powder Diffraction

The crystalline/amorphous state of the synthesised glasses was evaluated using X-ray powder diffraction (XRD) [18]. The diffractograms were collected on a

Bruker D8 Discover, operating with CuK radiation, in $\theta/2\theta$ mode, between 6° and 70° , with a step increment of 0.04° and an acquisition time of 1s per step.

3.4 Scanning Electron Microscopy

Scanning Electron Microscopy (SEM) was used to analyze the formation and morphology of calcium phosphate layers (*in vitro* bioactivity) at the surface of the cements after immersion in SBF at 7 and 14 days (non-immersed samples were used as controls). The micrographs were collected on a Leica Cambridge S360 microscope using a beam energy of 15.0 kV and a working distance (WD) of 19 mm. All the analysed samples were previously coated with gold to enhance its conductivity (Figure 6).

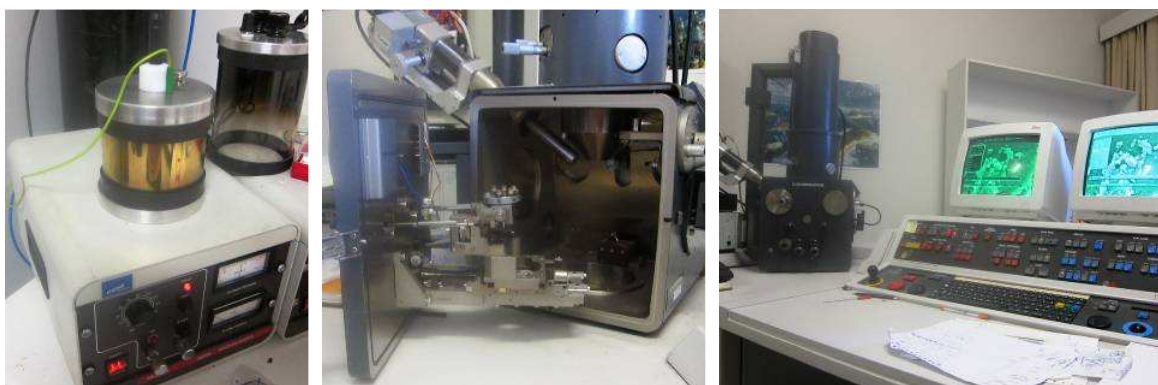


Figure 6: Gold deposition, microscope chamber and overall view of SEM microscope.

3.5 Micro-Computed Tomography

The cements samples were analysed by micro-Computed Tomography (micro-CT) in order to determine the polymer, glass and pore spatial distribution and volume percentages. The collection of images was performed in a micro-CT Skyscan 1072 (Skyscan, Belgium) operating with a voltage of 104 kV and with a current of 96 μ A (Figure 7). Upon image acquisition the noise was reduced using nRecon software. Afterwards, 200 sliced images were obtained using the CT-An program. These images were used to produce a 3D reconstructions with the same program (CT-An). Manipulating the image with a threshold of 40 to 80 for the glass and 80 to 140 for the polymer it was possible to separate the contribution of PAA and glass components to the cement volume, as well as the free pore volume [19].



Figure 7: Micro-Computed Tomography equipment.

3.6 Water uptake and weigh loss

3.6.1 Water uptake

Cement samples (prepared 24 h before testing to allow stabilization) were immersed in Phosphate Buffer Saline (PBS) solution at a ratio of 1:15 (sample mass : PBS volume) and inserted in a shaking water bath maintained at 37 °C and 60 rpm. In all the cases it was prepared three replicas of each sample that were collected during the study. Cement samples were collected at various time points (1, 2, 4, 8 and 12 weeks) and were washed with distilled water. The excess of water present in the surface of the cements was dried with paper and then the cements were immediately weighted.

The water uptake (WU) was calculated using the following equation [20]:

$$WU = \frac{(m_{tp} - m_f)}{m_f} \times 100$$

Equation 2

where, m_{tp} is the mass of the wet specimen at a specific time point and m_f is the mass of cement after drying at 37 °C to constant weight.

3.6.2 Weight loss

The weight loss (WL) was calculated during the water uptake (WU) tests. In the WL case, the cements were removed from the PBS solution at the same time intervals as the ones used for the WU (1, 2, 4, 8 and 12 weeks) and were dried in the oven, at 37 °C, until constant weight. The percentage of WL was calculated using the following equation:

$$WL = \frac{(m_f - m_i)}{m_i} \times 100 \quad \text{Equation 3}$$

where, m_f is the mass of the dried cement after its immersion in PBS and m_i is the mass of the dried cement before immersion in PBS.

4. Bioactivity assays

4.1 Preparation of Simulated Body Fluid and the cements samples

Simulated body fluid (SBF) is a solution that mimics the ion concentrations in the human plasma, as indicated in Table 3.

Table 3: Ionic concentration of the human blood plasma and the SBF solution.

Ions	Concentration in Blood plasma (mM)	Concentration in SBF solution (mM)
Na ⁺	142.0	142.0
K ⁺	5.0	5.0
Mg ²⁺	1.5	1.5
Ca ²⁺	2.5	2.5
Cl ⁻	103.0	147.8
HCO ₃ ⁻	27.0	4.2
HPO ₄ ³⁻	1.0	1.0
SO ₄ ²⁻	0.5	0.5

The preparation of SBF followed a specific protocol as detailed in the following steps:

- 1 L of distilled water was maintained in a bath at the temperature of 100 °C-150 °C and at 300-450 rpm;
- It was performed a temperature and pH control;
- The masses of each reagent was added in the order described in Table 4 to produce 2 L of SBF;
- The temperature of the solution was adjusted to 36.5 °C and the pH to 7.40;
- The solution was transferred to a volumetric flask and the volume was adjusted when the temperature reached 20 °C;
- After sterilization by filtration, the solution was stored at 5-10 °C.

Table 4: Quantities and sequence of the addition of each reagent in the protocol followed for the preparation of the SBF solution.

Sequence	Reagent	Quantity	Purity /%
1	NaCl	16.072 g	99.5
2	NaHCO ₃	0.704 g	99.5
3	KCl	0.450 g	99.5
4	K ₂ HPO ₄ ·3H ₂ O	0.460 g	99.0
5	MgCl ₂ ·6H ₂ O	0.622 g	98.0
6	HCl 1M	50 mL	-
7	CaCl ₂	0.586 g	95.0
8	Na ₂ SO ₄	0.144 g	99.0
9	TRIS	12.236 g	99.0
10	HCl 1M	25 mL	-

4.2 Bioactivity assay

Cement samples (prepared 24 h before testing to allow stabilization) were immersed in Simulated Body Fluid (SBF) solution at a ratio of 1:10 (sample mass : SBF volume) and inserted into an oven maintained at 37 °C. Cement samples (including three replicas per formulation and time point) were collected at two time points (7 and 14 days). The collected SBF solutions were filtered and stored in a controlled temperature room at 4 °C until further analysis.

4.3 Analysis of calcium and phosphorous concentration by inductive coupled plasma – optical emission spectroscopy

Inductive coupled plasma optical emission spectrometry (ICP-OES) was used to determine the calcium and phosphorous concentrations in the SBF solution before and after the immersion of the developed cements at 7 and 14 weeks (Figure 8). The higher ability of the cement to form a calcium phosphate layer in the surface of the cement (a measure of its *in vitro* bioactivity), higher is the reduction of the calcium and phosphorous concentrations in the SBF. The analytical methodology comprises the nebulisation of the SBF solutions into an oven maintained at a temperature between 6000 and 10000 K to atomize the chemical compounds. Afterwards, the samples' absorption at specific wavelengths ($\lambda=422.67$ nm for Ca and $\lambda=213.62$ nm for P) was measured and the Ca and P concentrations were determined using calibration curves previously obtained with standard solutions (Alfa Aesar).



Figure 8: ICP-OES analysis of the developed cements.

4.4 Energy-dispersive X-ray spectroscopy

The Energy-dispersive X-ray Spectroscopy (EDS) was used to analyse the surface elemental composition of the prepared cement samples before and after immersion in simulated body fluid (SBF) – bioactivity assays. For this purpose, a Link eXL-II Oxford spectroscope was used at an energy of 7.0 KeV. The EDS analysis was used to quantify the calcium and phosphorous present in the surface of the cements after immersion during 7 and 14 days in SBF. Prior to the analysis the samples were carbon coated to improve their conductivity (Figure 9).



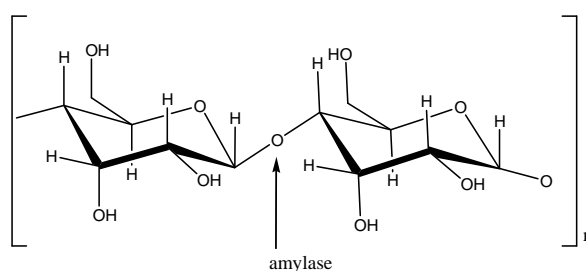
Figure 9: Carbon deposition of the analysed samples and EDS equipment.

5. Degradation studies

The kinetics and percentage of cement degradation are important parameters to evaluate their suitability as bone cements. In fact, it is expectable that the developed cements will be slowly reabsorbed and excreted from the body. The kinetics of this process should match the formation of new bone so that the loss of the cementing effect of the reabsorbed part will not impart a reduction of properties in the intervened portion of the bone. In this perspective, it was analysed the kinetics and percentages of weight loss of the developed cements (see water uptake and weight loss in section 3 of this chapter). Additionally, the degradation kinetics of the cements prepared with the addition of starch particles were analysed in the presence of a starch-specific enzyme, α -amylase.

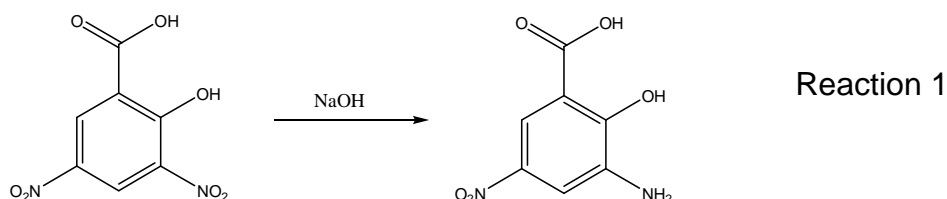
5.1 Enzymatic degradation – reducing sugars

The degradation of the starch-containing cements was tested in the presence of a starch-specific enzyme, α -amylase. This enzyme is known to hydrolyse the α -1,4-glycosidic linkages of polysaccharides (e.g. starch) to monosaccharides, such as, maltose and dextrans (scheme 1).



Scheme 1

Cement degradation was promoted by immersion of specimens in an enzyme containing solution (150 U/L) for different time periods, 0, 1, 2, 4, 8, and 12 weeks. At the specific time points, the solutions were analysed for the presence of reducing sugars. Their concentration was determined by the dinitrosalicylic acid (DNS) method. The 3,5-dinitrosalicylic acid is converted to 3-amino-5-nitrosalicylic acid in alkaline conditions according to the reaction 1.



This last compound (3-amino-5-nitrosalicylic acid) forms a complex with the reducing sugars, which presents an absorption peak at 540 nm. All the immersion solutions were analyzed in a UV-VIS spectrophotometer (microplate reader Synergie HT). Previous to the analysis a calibration curve was obtained using standard solutions of dextrose (Sigma-Aldrich), allowing the determination of the concentration of reducing sugars present in the immersion solutions.

6. Statistical methods

6.1 Dixon test (Q-test)

The Dixon test is an outlier test that informs if the minimum or the maximum value of a dataset from the same formulation may be rejected or not. The test is based on equation 4 and 5 and was used in the datasets obtained from the mechanical analysis.

$$Q_{\text{calculated}} = \frac{|x_2 - x_1|}{|x_n - x_1|}, \text{ for the minimum value} \quad \text{Equation 4}$$

$$Q_{\text{calculated}} = \frac{|x_n - x_{n-1}|}{|x_n - x_1|}, \text{ for the maximum value} \quad \text{Equation 5}$$

Where the data values are: $x_1, x_2, x_3 \dots x_{n-1}, x_n$.

Considering a specific probability (in our case 95 %) the $Q_{\text{tabulated}}$ is selected from the corresponding statistical table. If the $Q_{\text{calculated}} < Q_{\text{tabulated}}$ the value was not rejected within the given probability and if the $Q_{\text{calculated}} > Q_{\text{tabulated}}$ the value was rejected within the given probability.

6.2 Normality test

All the described statistics can only be applied if the datasets follow a normal distribution. Considering this fact, all the datasets were tested for normality using the Shapiro-Wilk analysis. This test indicates if the dataset is normally distributed at a 95 % probability. Considering the normal distribution, if the p-value was less than 0.05, it was considered that the dataset was not significantly drawn from a normally distributed population and if the p-value was higher than 0.05 the dataset was considered to be significantly drawn from a normally distributed population (Figure 10). All the tested datasets were in accordance with the normal distribution making it possible to perform a significance test (t-test) [21].

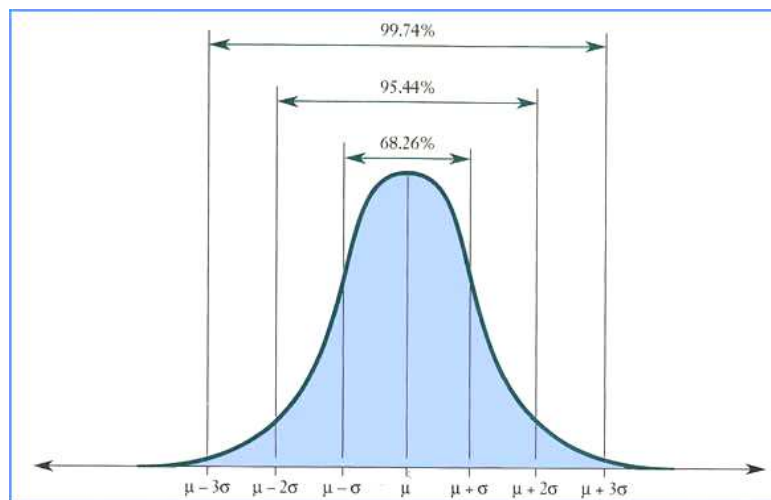


Figure 10: Scheme of normal distribution (adapted by <http://www.conferences.utah.edu/ishpssb/publicforum.html>).

6.3 t-test

With the t-test it was possible to analyse if the differences between the averages of the datasets are significantly or not. The t-test was employed in the analysis of the datasets obtained from the mechanical analysis, namely from the compressive strength (CS) and modulus (CM) of the cements. A comparison of the averages of the datasets is done considering a null hypothesis ($\text{mean1} - \text{mean2} = 0$). From the results it was possible to conclude if the differences between the averages are significant or not within a 95 % probability.

Bibliography

1. Wren, A., D. Boyd, and M. Towler, *The processing, mechanical properties and bioactivity of strontium based glass polyalkenoate cements*. Journal of Materials Science: Materials in Medicine, 2008. **19**(4): p. 1737-1743.
2. Pereira, D., et al., *Surface behaviour of high MgO-containing glasses of the Si-Ca-P-Mg system in a synthetic physiological fluid*. Journal of the European Ceramic Society, 2004. **24**(15-16): p. 3693-3701.
3. Boyd, D. and M. Towler, *The processing, mechanical properties and bioactivity of zinc based glass ionomer cements*. Journal of Materials Science: Materials in Medicine, 2005. **16**(9): p. 843-850.
4. Nicholson, J.W., *Chemistry of glass-ionomer cements: a review*. Biomaterials, 1998. **19**(6): p. 485-494.
5. De Barra, E. and R.G. Hill, *Influence of glass composition on the properties of glass polyalkenoate cements. Part III: influence of fluorite content*. Biomaterials, 2000. **21**(6): p. 563-569.
6. Hurrell-Gillingham, K., et al., *Devitrification of ionomer glass and its effect on the in vitro biocompatibility of glass-ionomer cements*. Biomaterials, 2003. **24**(18): p. 3153-3160.
7. Boyd, D., et al., *TEM analysis of apatite surface layers observed on zinc based glass polyalkenoate cements*. Journal of Materials Science, 2008. **43**(3): p. 1170-1173.
8. Dietrich, E., et al., *Effects of Mg and Zn on the surface of doped melt-derived glass for biomaterials applications*. Applied Surface Science, 2008. **255**(2): p. 391-395.
9. Hee-Gon Bang, S.-J.K.a.S.-Y.P., *Biocompatibility and the physical properties of bio-glass ceramics in the Na₂O-CaO-SiO₂-P₂O₅ system with CaF₂ and MgF₂ additives*. Journal of Ceramic Processing Research, 2008. **9**(6): p. 588-590.
10. Abou Neel, E.A., et al., *Bioactive functional materials: a perspective on phosphate-based glasses*. Journal of Materials Chemistry, 2009. **19**(6): p. 690-701.
11. Pires, R.A., et al., *The role of alumina in aluminoborosilicate glasses for use in glass-ionomer cements*. Journal of Materials Chemistry, 2009. **19**(22): p. 3652-3660.

12. Wren, A., et al., *The effect of glass synthesis route on mechanical and physical properties of resultant glass ionomer cements*. Journal of Materials Science: Materials in Medicine, 2009. **20**(10): p. 1991-1999.
13. Brauer, D.S., et al., *Fluoride-containing bioactive glasses: Effect of glass design and structure on degradation, pH and apatite formation in simulated body fluid*. Acta Biomaterialia, 2010. **6**(8): p. 3275-3282.
14. Silva, G.A., et al., *The effect of starch and starch-bioactive glass composite microparticles on the adhesion and expression of the osteoblastic phenotype of a bone cell line*. Biomaterials, 2007. **28**(2): p. 326-334.
15. Xu, X. and J.O. Burgess, *Compressive strength, fluoride release and recharge of fluoride-releasing materials*. Biomaterials, 2003. **24**(14): p. 2451-2461.
16. Xie, D., et al., *Mechanical properties and microstructures of glass-ionomer cements*. Dental Materials, 2000. **16**(2): p. 129-138.
17. Yli-Urpo, H., et al., *Compressive strength and surface characterization of glass ionomer cements modified by particles of bioactive glass*. Dental Materials, 2005. **21**(3): p. 201-209.
18. Garcia, L.d.F.R., et al., *Synthesis and biocompatibility of an experimental glass ionomer cement prepared by a non-hydrolytic sol-gel method*. Brazilian Dental Journal, 2010. **21**: p. 499-507.
19. Nomoto, R., et al., *Effect of mixing method on the porosity of encapsulated glass ionomer cement*. Dental Materials, 2004. **20**(10): p. 972-978.
20. Boesel, L.F., H.S. Azevedo, and R.L. Reis, *Incorporation of α -Amylase Enzyme and a Bioactive Filler into Hydrophilic, Partially Degradable, and Bioactive Cements (HDBC)s as a New Approach To Tailor Simultaneously Their Degradation and Bioactive Behavior*. Biomacromolecules, 2006. **7**(9): p. 2600-2609.
21. Miller, J.N.a.M., J. C., *Statistics and Chemometrics for Analytical Chemistry - 5th ed*. 2005.

Chapter III

Aluminum-free glass ionomer bone
cements with enhanced bioactivity
and biodegradability

Aluminum-free glass ionomer bone cements with enhanced bioactivity and biodegradability

F. O. Gomes^{1,2*}, R. A. Pires^{1,2}, R. L. Reis^{1,2}

¹ 3B's Research Group – Biomaterials, Biodegradables and Biomimetics, University of Minho, Headquarters of the European Institute of Excellence on Tissue Engineering and Regenerative Medicine, AvePark, 4806-909 Taipas, Guimarães, Portugal

² ICVS/3B's - PT Government Associate Laboratory, Braga/ Guimarães, Portugal

*Corresponding author. Address: 3B's Research Group – Biomaterials, Biodegradables and Biomimetics, University of Minho, Headquarters of the European Institute of Excellence on Tissue Engineering and Regenerative Medicine, AvePark, 4806-909 Taipas, Guimarães, Portugal

E-mail: filipa.gomes@dep.uminho.pt

Abstract

Glass ionomer cements (GICs) are used in dentistry and their application as bone cements have been mainly limited by the presence of cytotoxic aluminium (Al) in the glass composition. We developed Al-free glasses of general composition 0.340SiO_2 : 0.300ZnO : $(0.250-x-y)\text{CaO}$: $x\text{SrO}$: $y\text{MgO}$: $0.050\text{Na}_2\text{O}$: $0.060\text{P}_2\text{O}_5$ ($x, y = 0.000$ or 0.125) and tested them for their cement forming ability in the presence of polyacrylic acid (PAA) and water. The influence of the type of cations present in the glass (Ca^{2+} , Sr^{2+} and Mg^{2+}); the PAA molecular weight (M_w) and the glass particle size in the cement final properties (mechanical behaviour and bioactivity) were evaluated. Enhanced compressive strength (25 ± 5 MPa) and modulus (492 ± 17 MPa) was achieved with PAA of 50 kDa and glass particle sizes between 63-125 μm . The GICs' *in vitro* bioactivity was tested in simulated body fluid (SBF) and their response analysed by ICP, SEM and EDS. Enhanced bioactivity was observed for glass composition $x=0.125$; $y=0.000$, presenting a surface calcium (Ca)/ phosphorous (P) ratio of 1.6 (similar to hydroxylapatite) and a surface morphology consistent with a CaP coating. Starch was added to the cement formulation $x=0.125$; $y=0.000$ (at 0.050 and 0.250 weight proportions) in order to enhance its biodegradability (tested by immersion in phosphate buffer saline in the presence of α -amylase). The results obtained from the determination of the reducing sugars in the degradation solution indicate that starch only starts to degrade after 8 weeks of immersion. Our studies indicate that it is possible to formulate Al-free GIC compositions with potential to be used as bone cements.

Keywords: glass ionomer cements, bone cements, mechanical properties, bioactive, biodegradable

1. Introduction

Wilson and Kent created the first glass-ionomer cement (GIC), in the early 1970s [1, 2]. GICs are prepared through the mixing of a glass powder, usually a calcium fluoroaluminosilicate, with polyacrylic acid (PAA) and water. The curing reactions usually occur in two phases designated as gelation and maturation [3]. During gelation the acidic PAA attacks the glass particles at their basic sites, promoting the release of cations, e.g. 5-coordinated and 6-coordinated aluminium (Al) in the ionic form Al^{3+} , Ca^{2+} , etc., from the glass to the cement matrix [4]. This process is followed by the maturation phase that includes the leaching of covalently bounded 4-coordinated Al (slower process due to its more stable position in the glass structure) and the ionic cross-linking of the PAA chains by the leached cations. These two cements curing phases generates the final GIC structure - a composite of cross-linked PAA reinforced with the reacted glass particles [5].

Initial application of this type of cements was in dentistry due to their unique properties, namely, its strong adhesion to the hydroxylapatite present in dentin and its anti-cariogenic potential [1, 6-8]. Initial drawbacks of conventional GICs comprised, e.g. sensitivity to moisture during initial hardening, poor mechanical properties, among others. Optimization of their formulations resulted in conventional and modified GICs (e.g. resin-modified GICs) with enhanced behaviour [9, 10]. GICs continue to be mainly applied in the dentistry field, although, some tests have been made to use them as bone cements. These attempts revealed to be unsuccessful due to Al cytotoxicity present in the glass composition and in the cement matrix [11, 12]. More recently, a series of studies [13-15] have been dedicated to eliminate Al from the cement formulation in order to avoid its deleterious cytotoxic effect. In fact, Towler and co-workers already shown that Al-free glass particles of the ternary system calcium-zinc-silicates [16] and quaternary system calcium-strontium-zinc-silicates [17, 18] possess cement-forming ability. These glass compositions always included low calcium/strontium fractions (cumulative values below 0.16) limiting the glass reactivity towards the PAA. In this study we hypothesise that: 1) the increase of the glass basic sites might increment the glass reactivity inducing an enhancement of the GIC mechanical behaviour; 2) the inclusion of higher fractions of CaO/SrO/MgO might improve the GIC *in vitro* bioactivity; 3) it is

expectable that the type of divalent cations (group II) included in the glass formulations (i.e. Ca^{2+} , Sr^{2+} and Mg^{2+}) will influence the cement final properties (e.g. mechanical behaviour, bioactivity, etc.); and 4) the addition of starch to the cement formulation improves the GIC biodegradability.

2. Materials and methods

2.1 Materials – Glass synthesis

Glass formulations of general formula $0.340\text{SiO}_2: 0.300\text{ZnO}: (0.250-x-y)\text{CaO}: x\text{SrO}: y\text{MgO}: 0.050\text{Na}_2\text{O}: 0.060\text{P}_2\text{O}_5$ (where x and $y = 0.125$ or 0.000) were prepared by melt quenching using appropriate proportions of glass precursors (Table 1). For this purpose, silica (Merck), zinc oxide (Sigma), magnesium oxide (Sigma, 98 %), calcium carbonate (Sigma, 99 %), strontium carbonate (Sigma, 98 %), sodium hydrogenocarbonate (Riedel de-Haen, 99.7 %) and diammonium hydrogenophosphate (Sigma, 98 %) were grounded with a pestle and mortar transferred to a crucible and fired to 300 °C to release ammonia, 650 °C to allow the release of carbon dioxide and to 1300 °C to produce the melt.

Table 1: Composition of the synthesized glass formulations (mol %).

Component	G1*	G2	G3	G4	G5	G6
SiO₂	0.340	0.340	0.340	0.340	0.340	0.340
ZnO	0.300	0.300	0.300	0.300	0.300	0.300
MgO	0.250	-	-	0.125	-	0.125
CaO	-	0.250	-	0.125	0.125	-
SrO	-	-	0.250	-	0.125	0.125
Na₂O	0.050	0.050	0.050	0.050	0.050	0.050
P₂O₅	0.060	0.060	0.060	0.060	0.060	0.060

*G1 – Not possible to produce an homogeneous melt under the used experimental conditions.

Glass blocks were immersed in liquid nitrogen and grounded with a pestle and mortar. The glass particles were separated by size using an Analytical Sieve Shaker (Retsch AS200) for 5 min at 60 rpm. With this procedure it was possible to collect three different fractions (with particle of sizes <63 µm, between 63-125 µm and between 125-250 µm) for each glass composition.

2.2 Cement preparation

Cements were prepared mixing the glass powder with PAA and water at appropriate proportion (55: 21: 24 by mass). PAA of different molecular weights (M_w s) were tested, namely, 50 kDa (PolySciences); 450 kDa (Sigma-Aldrich) and 1250 kDa (Sigma-Aldrich). The cement formulation that presented higher mechanical performance was modified to enhance its biodegradability. To this purpose it was added corn starch (Sigma) to formulations in weight percentages of 5 % and 25 %. All the cement pastes (immediately after mixing) were shaped in a Teflon mould to produce cylindrical specimens of 6 mm diameter and 11 mm height.

2.3 Glass and cement characterization

2.3.1 X-Ray Diffraction

The crystalline/amorphous state of the synthesized glass formulations was evaluated by x-ray powder diffraction (XRD). Diffractograms were collected on a Bruker D8 Discover, operating with Cu K α radiation, in $\theta/2\theta$ mode, between 6° and 70°, with a step increment of 0.04° and an acquisition time of 1 s per step.

2.3.2 Fourier Transform Infrared spectroscopy

The Fourier Transform Infrared (FTIR) spectra of the glasses and cements were collected using KBr (Sigma, 99%+) pellets on a Shimadzu IR-Prestige 21 spectrometer under transmittance mode, between 4400-400 cm⁻¹, using a resolution of 4 cm⁻¹ and 32 scans.

2.3.3 Mechanical testing

The compressive strength (CS) and modulus (CM) of the cements were evaluated. The developed cement formulations were mechanically tested under compression loading on an Instron 5540 (Instron, USA) using a 1 kN load cell and 2 mm/min of crosshead speed. Six cylindrical specimens of each formulation were tested 1 day after preparation. The specimen compressive strength (CS) was calculated according to equation 1:

$$CS = \frac{4p}{\pi d^2} \quad (1)$$

where p is the maximum applied load (N) and d is the diameter of the sample (mm).

The compressive modulus (CM) was calculated as the initial slope (elastic regime) of the stress-strain curves of each cement specimen.

Averages were calculated for the CS and CM of each cement formulation and the normality of the data distribution was confirmed using the Shapiro-Wilk test. Significant differences (95 % probability) between the cement formulations were calculated using the t-test.

2.4 Bioactivity tests

2.4.1 In vitro bioactivity

Cement formulations were immersed in Simulated Body Fluid (SBF, prepared according to a previously established procedure [14]) during 7 and 14 days. At these specific time points, the specimens were collected from the solutions. The calcium (Ca) and phosphorous (P) concentrations of the initial SBF and immersion solutions were analyzed by Inductive Coupled Plasma – Optical Emission Spectroscopy (ICP-OES) and the elemental composition and morphology of the immersed and non-immersed cement surfaces were evaluated by Energy Dispersive X-ray spectroscopy (EDS) and Scanning Electron Microscopy (SEM).

2.4.2 Inductive coupled plasma – optical emission spectroscopy

ICP-OES was used to determine the Ca and P concentrations in the SBF solutions before and after the immersion of the developed cements. The samples' absorption at specific wavelengths ($\lambda=422.67$ nm for Ca and $\lambda=213.62$ nm for P) was measured and the Ca and P concentrations were determined from the calibration curves previously obtained with standard solutions (Alfa Aesar).

2.4.3 Energy-Dispersive x-ray Spectroscopy

The Energy-Dispersive x-ray spectroscopy (EDS) was used to quantify the Ca and P present in the surface of the cements. A Link eXL-II Oxford Spectroscope was used at an energy of 7.0 keV and the samples were carbon coated to improve their conductivity.

2.4.4 Scanning Electron Microscopy

Micrographs of the cement samples were collected on a Leica Cambridge S360 microscope using a beam energy of 15.0 kV and a working distance (WD)

of 19 mm. All the samples were previously coated with gold and the morphology of the CaP layers was verified after 7 and 14 days of immersion in SBF.

2.5 Water uptake and weigh loss

Cement samples (prepared 24 h before testing) were immersed in Phosphate Buffer Saline (PBS) solution at a ratio of 1:15 (sample mass: PBS volume) and inserted in a shaking water bath maintained at 37 °C and 60 rpm. Cement samples were collected at various time points (1, 2, 4, 8 and 12 weeks). They were washed with distilled water, the excess water present in the surface was dried with paper and the samples were immediately weighted. The water uptake (WU) was calculated using the equation 2.

$$WU = \frac{(m_{tp} - m_f)}{m_f} \times 100 \quad (2)$$

where, m_{tp} is the wet mass at the specific time point and m_f is the mass of cement after drying at 37 °C to constant weight.

The weight loss (WL) was calculated during the water uptake (WU) tests. In the WL case, the cements were removed from the PBS solution at the same time intervals as the ones used for the WU (1, 2, 4, 8 and 12 weeks) and were dried into the oven, at 37 °C, until constant weight. The percentage of WL was calculated using the equation 3.

$$WL = \frac{(m_f - m_i)}{m_i} \times 100 \quad (3)$$

where, m_f is the mass of the dried cement after its immersion in PBS and m_i is the mass of the cement before immersion in PBS.

2.6 Degradation tests

The degradation of the starch-containing cements was tested in the presence of a starch-specific enzyme, α -amylase. This enzyme is known to hydrolyse the α -1,4-glycosidic linkages of polysaccharides (e.g. starch) to monosaccharides, such as, maltose and dextrans.

Cement degradation was promoted by immersion of specimens in an enzyme containing solution (150 U/L) for different time periods, 0, 1, 2, 4, 8, and 12

weeks. At the specific time points, the solutions were analysed for the presence of reducing sugars. Their concentration was determined by the dinitrosalicylic acid (DNS) method. The 3,5-dinitrosalicylic acid is converted to 3-amino-5-nitrosalicylic acid in alkaline conditions. This last compound (3-amino-5-nitrosalicylic acid) forms a complex with the reducing sugars, which presents an absorption peak at 540 nm. All the immersion solutions were analyzed in a UV-VIS spectrophotometer (microplate reader Synergie HT). Previous to the analysis a calibration curve was obtained using standard solutions of dextrose (Sigma-Aldrich, nd), allowing the determination of the concentration of reducing sugars present in the immersion solutions.

2.7 Micro-Computed Tomography

The cement samples were analysed by micro-Computed Tomography (micro-CT) in order to determine the polymer, glass and pore spatial distributions and volume percentages. The collection of images was performed in a micro-CT Skyscan 1072 (Skyscan, Belgium) operating with a voltage of 104 kV and with a current of 96 μ A. Upon image acquisition the noise was reduced using nRecon software. Afterwards, 200 sliced images were obtained using the CT-An program. These images were used to produce a 3D reconstruction with the same program (CT-An). Manipulating the image with a threshold of 40 to 80 for the glass and 80 to 140 for the polymer it was possible to separate the contribution of these components to the cement volume, as well as the free pore volume.

3. Results and discussion

3.1 Glass characterization

3.1.1 X-Ray Diffraction

The XRD diffractograms of all the synthesised glass compositions presents the predominance of the amorphous state with a low contribution of crystalline phases only in the cases of samples G4 and G6 (see Figure 1).

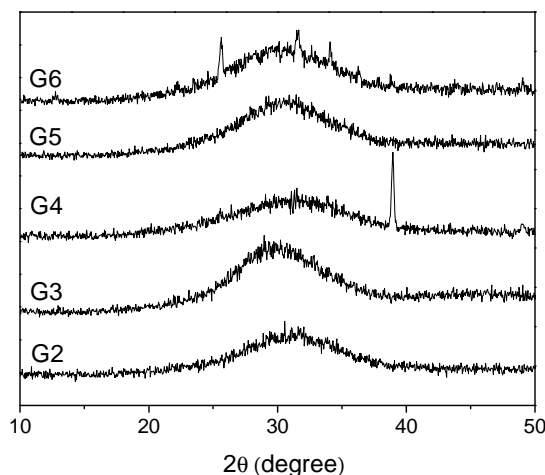


Figure 1: X-ray powder patterns of the synthesised glass formulations.

3.2 Cement characterization

3.2.1. Chemical characterization

FTIR spectra of the cement samples (cured during 24 h) were used to characterize their curing reactions and chemical structure. As an example, Figure 2 presents the FTIR spectra of PAA, glass G5 and cement C5.

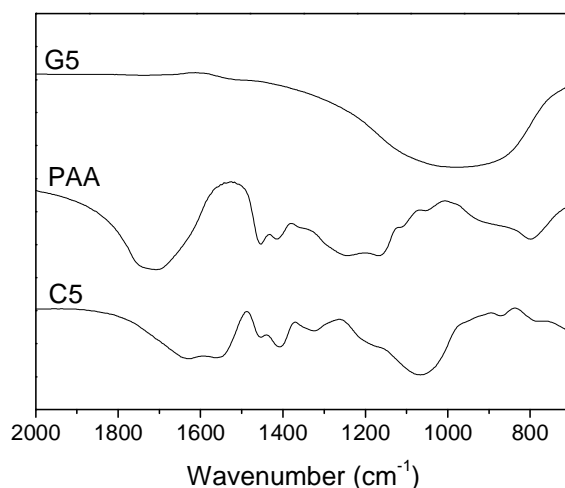


Figure 2: FTIR spectra of PAA, glass G5 and cement C5

It is known that the cement curing reactions comprises an acid attack promoted by the PAA carboxylic acids on the surface layer of the glass particles that partially leaches its cations to the cement matrix. These leached cations crosslink the polymeric chains (at the COO^- groups from the PAA) through the formation of ionic linkages [3]. In fact, the PAA, glass and cement FTIR spectra

(Figure 2) are consistent with this reaction model. Upon acid attack the PAA COOH stretching at 1750 cm^{-1} (observed before the curing reaction) is shifted to two peaks (symmetric and asymmetric stretching between 1640 cm^{-1} and 1550 cm^{-1}) of its ionized form (COO^-).

3.2.2 Mechanical testing

a) Influence of glass particle size and PAA molecular weight on the cement mechanical behaviour.

The influence of the glass particle size and the PAA molecular weight (M_w) on the mechanical behaviour of the cement (CS and CM) was also studied. To this purpose, three glass powder fractions (using G5) with different particle size distributions were obtained by sieving (i.e. $<63\text{ }\mu\text{m}$; $63\text{ }\mu\text{m}<x<125\text{ }\mu\text{m}$ and $125\text{ }\mu\text{m}<x<250\text{ }\mu\text{m}$) and three PAA samples of different M_w s (50 kDa, 450 kDa and 1250 kDa) were tested. The CS and CM values obtained with the cements prepared with the sieved glass powders and the PAA samples of different M_w are presented in Figure 3.

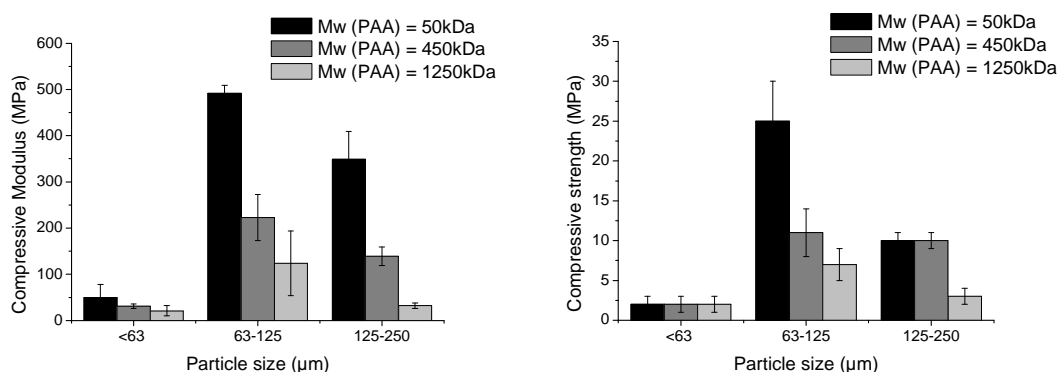


Figure 3: Compressive modulus (CM) and compressive strength (CS) of the cements prepared with the different particle sizes of glass powder and PAA M_w s.

Higher CS and CM values were obtained using PAA of 50 kDa and glass particle sizes between $63\text{ }\mu\text{m}$ and $125\text{ }\mu\text{m}$. In all the cases, when the glass particle size distribution or PAA M_w deviated from these optimal conditions, CM decreased significantly. In the case of the CS, not always it was observed a significant decrease, although, it was clear that the above mentioned optimal conditions yielded a cement formulation with enhanced CS [19, 20].

It was observed that a proper mixing of the cement paste would necessitate more water when the glass particle sizes are $<63\text{ }\mu\text{m}$. Although, other reports

[21] suggest that lower particle sizes would be beneficial for the cement mechanical properties. From our results it is possible to conclude that this relation is not universal and that the optimal glass particle sizes might vary with the glass composition. In fact, it is reasonable to assume that the higher the reactivity of the glass particles the higher should be the glass particle sizes (and consequently lower the surface area). If low particle sizes are used on glasses with high reactivity towards PAA their reaction is so fast that it is not possible to produce an homogeneous cement paste. In these cases the cement's working time is too short to allow its application in the cementation of bone and to yield enhanced mechanical performance.

b) Influence of the composition of each cement in the mechanical behaviour

In Figure 4 is presented the CM and CS obtained for the cement formulations prepared using the synthesised glasses (with particle size between 63 and 125 μm), PAA (50 kDa) and water.

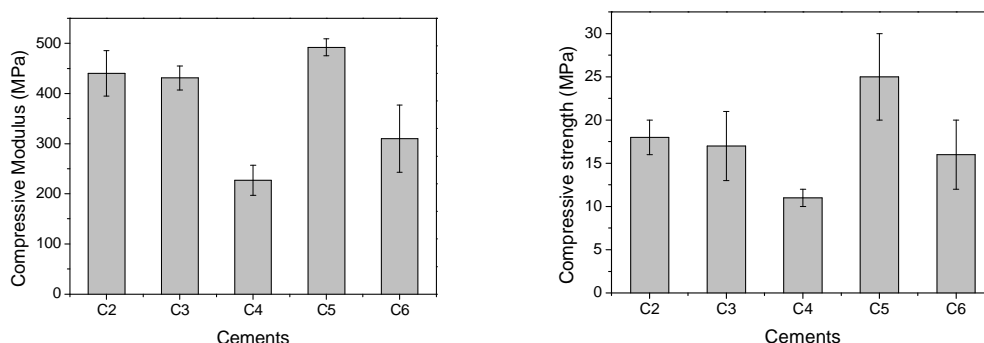


Figure 4: Compressive modulus (CM) and compressive strength (CS) of the developed cements.

Analysing the results obtained for the CM values it is clear the existence of two groups of formulations: group 1 composed by C4 and C6 that present lower CM; and group 2 composed by C2, C3 and C5 that exhibit higher CM. No significant differences were observed within each group, although, significant variations (95 % probability) were observed between the samples of the two groups. It is interesting to notice that lower CM is obtained for the cements prepared with glasses that presented MgO in the composition.

The mechanical analysis was complemented with the determination of the CS of the same cement formulations. From the three cements that presented

higher CM (C2, C3 and C5) the only one that presented a significantly higher mechanical resistance was C5. Overall, it presented a CM of 492 ± 17 MPa and a CS of 25 ± 5 MPa.

3.2.3 *In vitro* bioactivity

The ability of the cements to promote the formation of calcium phosphate (CaP) layers on their surface (in the presence of SBF) was used as a measure of their *in vitro* bioactivity. At a first stage cement samples were immersed in SBF for 7 and 14 days. ICP-OES was used to monitor the Ca and P concentration in the SBF solution before and after the cement immersion. Table 2 summarizes the Ca and P concentrations as percentage of the concentration in the original SBF.

Table 2: Ca and P concentrations in the SBF solutions after 7 and 14 days of immersion of GIC samples. Values are presented as percentage of the concentrations present in the original SBF, used as reference.

Samples	7 days		14 days	
	% Ca	% P	% Ca	% P
SBF	100.00	100.00	100.00	100.00
C2	63.04	62.96	64.13	59.26
C3	21.74	51.85	21.74	51.85
C4	52.17	40.74	57.61	40.74
C5	42.39	55.56	40.22	48.15
C6	18.48	51.85	20.65	59.26

The results clearly show a decrease of the Ca and P concentrations in the SBF for all the cement samples. The larger variations on the Ca were observed for C3 and C6, although, these are not accompanied by the P concentrations. In fact, the reduction in the P (concentrations between 40 % and 63 %) are levelled in all the cement formulations. In this case it is not noticed any specific trends.

ICP-OES of the immersion solution is an indirect method to determine the ability of the cements to produce CaP. The direct analysis of the elemental composition of the surfaces of the cements (after immersion in SBF for 7 and 14 days) was done using EDS (Figure 5).

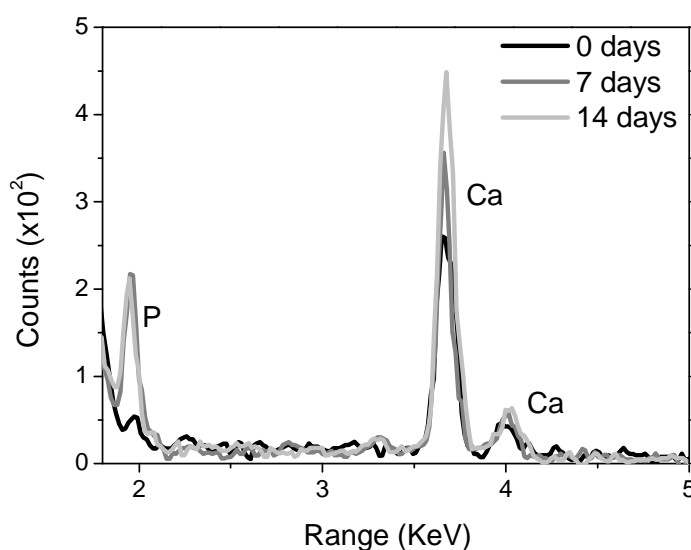


Figure 5: EDS spectra the surface of cement C5 immersed in SBF for 7 and 14 days (spectrum of non-immersed cement shown as reference – 0 days).

From the EDS spectra it was possible to collect the Ca and P concentrations in the cement surfaces (Table 3). It is known that biomaterials with high bioactivity present thicker CaP layers and these layers present the hydroxyapatite crystalline form. It is also known that the Ca/P ratio for hydroxyapatite is, approximately, 1.62 [22, 23]. In this perspective, the closer the Ca/P ratio is to the hydroxyapatite ratio the higher is the bioactivity of the cement. Under this assumption, the cement sample C5 presented Ca/P ratios of 1.8 and 1.6 at 7 and 14 days of immersion in SBF, respectively. From all the tested formulations, the C5 Ca/P values were the closest to hydroxyapatite, being considered as the one that presented highest bioactivity.

Table 3: Ca/P ratio of all cements after 7 and 14 days.

Cement	7 days			14 days		
	Ca	P	Ca/P	Ca	P	Ca/P
C2	0.83	1.20	0.70	2.30	1.97	1.17
C3	1.20	1.24	0.97	1.88	1.31	1.43
C4	1.48	0.99	1.49	0.79	1.14	0.70
C5	1.26	0.70	1.79	2.19	1.42	1.55
C6	0.53	0.74	0.71	0.45	0.58	0.77

Ca/P of hydroxyapatite 1.62.

In order to complement the analysis, SEM was used to monitor the morphology of the CaP layers (cement C5 presented in Figure 6 as an example).

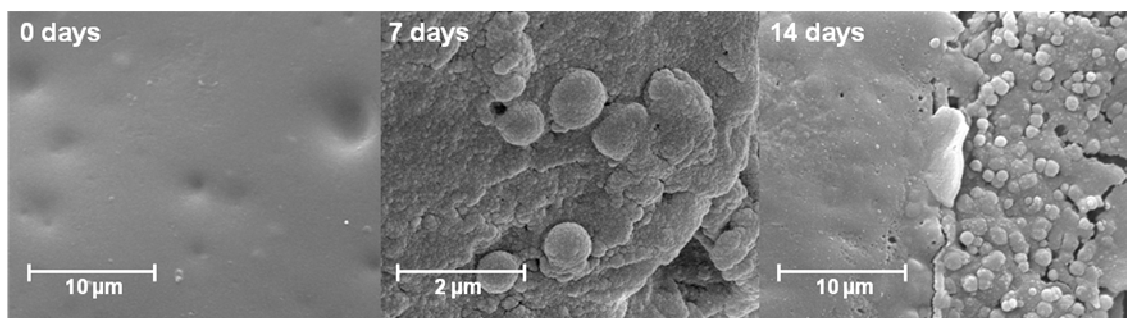


Figure 6: SEM micrographs of cement C5 before and after immersion in SBF for 7 and 14 days.

SEM analysis demonstrated the change in the cement morphology upon SBF immersion. Before immersion the cement surface is smooth without CaP crystals, while after 7 and 14 days of immersion it is possible to observe the formation of CaP layers that in some cases present the cauliflower form, characteristic of hydroxyapatite.

Considering the *in vitro* bioactivity and mechanical testing results it was clear that cement C5 exhibited properties that best match their use as bone cement. In this perspective, this composition was selected for subsequent analysis and testing.

3.2.4 3D distribution of glass, PAA and porosity of C5 cement

Micro-CT was used to obtain the spatial distribution of the glass particles, PAA and porosity of the cement sample that exhibited higher mechanical performance and bioactivity (C5).

The analysis of the C5 micrographs (Figure 8) indicates a higher predominance of PAA in the surface of the cement than in the bulk. This is assigned to the moulding process executed for all the formulations before the analysis. Additionally, using the micrographs it was possible to determine the porosity of the cement samples. In the case of cement C5 it was calculated a porosity of, approximately, 35 % in volume.

3.2.5 Water uptake and weight loss

The cement that presented higher mechanical performance and bioactivity (C5) was again chosen to study the water uptake and weight loss of this type of cement formulations. In this case, C5 presented an initial water uptake of 22 % that stabilised 1 week after immersion, reaching a plateau between 22 % and 25 % during all the subsequent time period (12 weeks) (Figure 9 and Figure 10).

3.3 Addition of starch to the cement formulation

3.3.1 Mechanical testing

Cement sample C5 was prepared with two different percentages of starch (5 % and 25 %). As expected the incorporation of starch as filler in the cement formulations produced a decrease of its mechanical performance (see Figure 7).

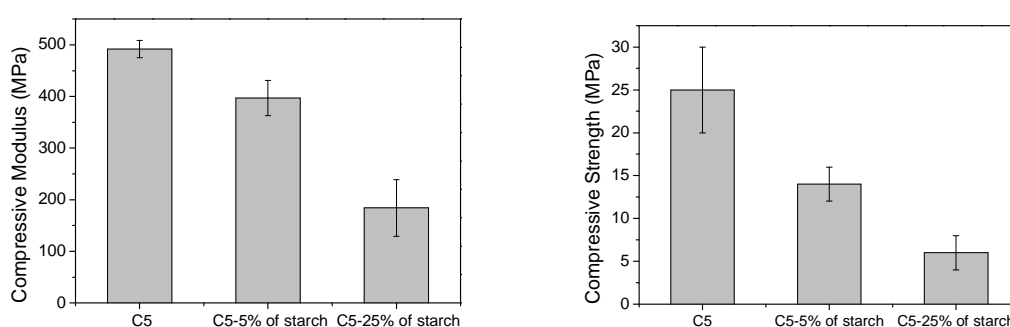


Figure 7: Compressive strength (CS) and compressive modulus (CM) for the cements as a function of the percentage of starch in the formulations.

It is always observed a significant decrease on the CS and CM when starch is included in the formulation. In the case of CM this decrease is limited to, approximately, 20 % when 5 % of starch is added, although, when higher percentages of starch are used the reduction of CM is higher than 65 %. CS is more sensitive to the inclusion of starch. In fact, the addition of 5 % of starch produced a decrease of, approximately, 50 % of the CS of the initial cement formulation.

3.3.2 3D distribution of the glass, polymers and porosity on the starch-containing cements

The 3D micrograph of the C5 cement with 0 %, 5 % and 25 % of starch is presented in Figure 8. It is clearly noticed a reduction of the PAA domains (lighter regions) in the surface of the cement with the increase of starch content. In fact, it was observed an increase of viscosity of the cement paste with the addition of starch. Under these conditions it is expectable a lower mobility of the PAA during the moulding process, limiting its diffusion to the surface of the cement.

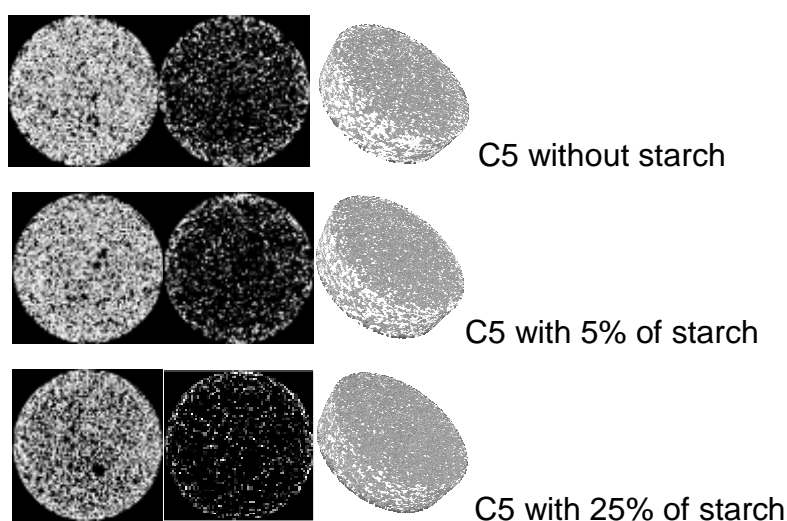


Figure 8: Micro-CT bidimensional image and 3D image of C5 cement without starch and with 5 % and 25 % of starch.

With the acquired micrographs it was also possible to determine the porosity of the cement samples. The inclusion of starch into the cement formulation produced an increase of porosity from, approximately, 35 % to 43 %. It is clear that the packing of the starch particles within the cement structure induces the appearance of a significant free-volume that is the responsible for the increment of the cement porosity. When the starch percentage was increased from 5 % to 25 % no significant variations in the porosity was observed. In fact, the porosity is maintained within the 41 % and 42 % range.

3.3.3 Water uptake and weight loss

The WU and WL of the C5 cement with 0 %, 5 % and 25 % of starch was determined through the immersion of the cement samples in PBS (at the

physiological pH, 7.4) during different time periods (up to 12 weeks). The solution pH value was monitored throughout the experiment. It was observed a reduction of the pH from the initial 7.4 to 7.0. This result was attributed to the partial solubilisation of the PAA present in the cement formulations.

In relation to the WU all the cements presented a similar general trend. It is observed an initial uptake during the first week (between 20 % and 37 %) that is maintained throughout the timeframe of the experiment (Figure 9). The inclusion of starch in the cement composition increased the hydrophilicity of the cements and their WU values change from, approximately, 25 % (C5 without starch) to 28 % (C5+5 % starch) and 35 % (C5+25 % starch). The enzymatic environment did not induce any observable differences in the WU of the cements when compared to the cements immersed in PBS without α -amylase.

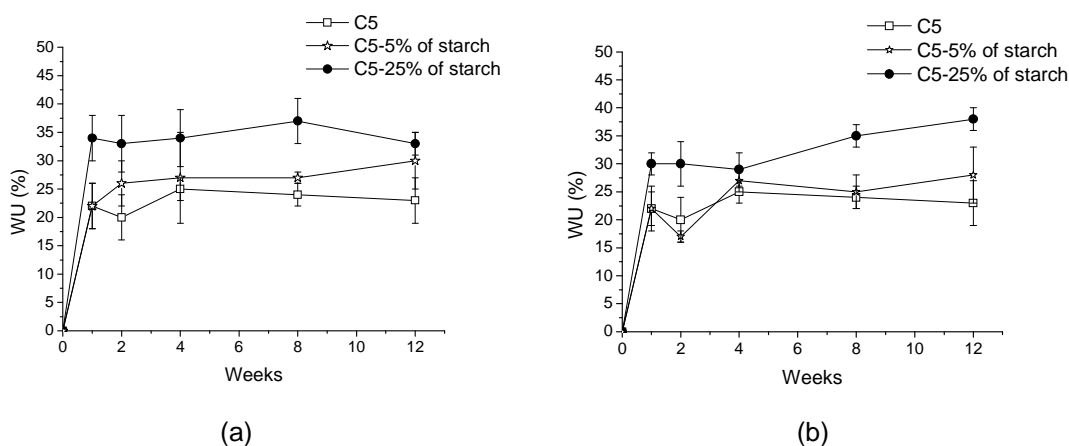


Figure 9: Water uptake (WU) of the cements under PBS (a) and PBS + α -amylase (b) during 12 weeks.

The WLs of the cement C5 with and without the addition of starch are similar (Figure 10). In fact it is observed an initial WL between 10 % and 16 % during the first week of experiment that is maintained throughout all the timeframe of the experiment. Comparing the WL values after 12 weeks of immersion, the observable differences between the samples are not significant (between 11 % and 13 % of WL). When the same formulations were immersed in PBS solution in the presence of α -amylase it was expectable to observe a higher decrease of WLs in the starch containing formulations. Although, the results indicate that the enzymatic medium has an inhibitory effect on the processes that are responsible for the WL of the GICs.

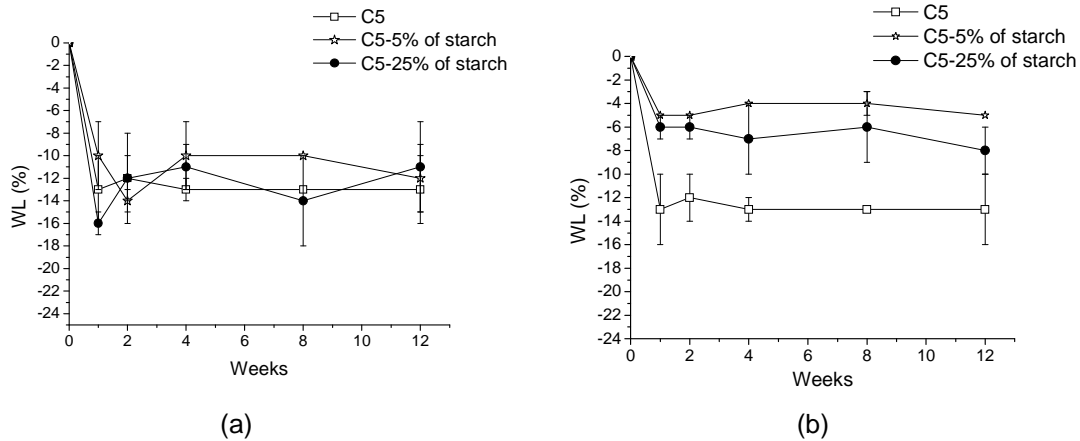


Figure 10: Weight loss (WL) of the cements under PBS (a) and PBS + α -amylase (b) during 12 weeks.

In fact, it is clear from our results that the WL is reduced to approximately half when enzymatic medium is used. Under these not expectable results, it is relevant to evaluate if the starch is actually degrading into reducing sugars or not.

3.3.4 Degradation tests

Starch was added to cement C5 in order to enhance the cement degradability, although, WL studies under enzymatic medium showed that the cement WLs were diminished. In this perspective the enzyme activity and starch degradation rate was monitored through the measurement of the concentration of reducing sugars released from the cements into the PBS.

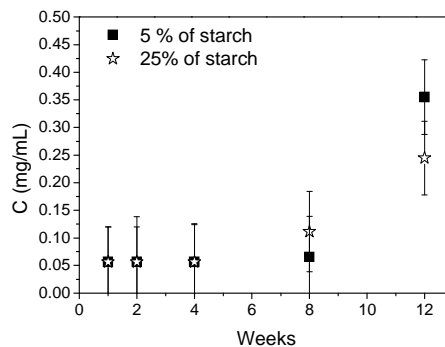


Figure 11: Concentration of reducing sugars in the cements (with 5% and 25% of starch) after immersion in PBS during 12 weeks.

The concentration of the reducing sugars increased as a function of time after the 8 and 12 weeks and no significant differences were observed for the cements in the first three time points (1, 2 and 4 weeks) (see figure 11). Apparently, the starch particles are only in contact with the enzymatic medium after the eighth week of immersion. Until this time point it they appear to be entrapped in the GIC structure without any connection with the immersion solution.

Considering the increasing of the concentration of reducing sugars in the enzymatic medium (after the 8th week of immersion) there is a clear indication that the addition of starch to the GIC formulations induces an enhanced biodegradability at a larger timeframe than expectable.

4. Conclusions

Our results demonstrate that it was possible to prepare Al-free glass-ionomer cement formulations using glasses of general formula $0.340\text{SiO}_2: 0.300\text{ZnO}: (0.250-x-y)\text{CaO}: x\text{SrO}: y\text{MgO}: 0.050\text{Na}_2\text{O}: 0.060\text{P}_2\text{O}_5$ (where x and $y = 0.000$ or 0.125). The inclusion of MgO revealed not appropriate for the achievement of cement with enhanced mechanical performance and bioactivity. Although, the combination of SrO and CaO (G5, $x = 0.125$; $y = 0.000$) produced a glass composition that generated cements with enhanced mechanical performance ($\text{CS} = 25 \pm 5$ MPa and $\text{CM} = 492 \pm 17$ MPa) and bioactivity ($\text{Ca/P} = 1.6$), with limited WU (approximately, 20 %) and WL (approximately, 13 %).

The optimized C5 cement formulation presented porosities in the range of 35 % that could be increased to 43 % with the inclusion of starch in the cement formulation. Moreover, the presence of reducing sugars in the enzymatic degradation solution after 8 weeks of testing indicates the existence of improved biodegradability at a longer timeframe than expected.

Our work demonstrates that it is possible to design Al-free glass-ionomer cement formulations that exhibit suitable mechanical performance and bioactivity. The elimination of the Al from the glass generates cement formulations suitable to be used as bone cements. The collected data is also

consistent with the possibility to develop formulations with improved biodegradability if starch (up to 25 %) is added to the cement formulation.

Bibliography

1. Wilson, A.D. and B.E. Kent, *Glass-Ionomer Cement, a New Translucent Dental Filling Material*. Journal of Applied Chemistry and Biotechnology, 1971. **21**(11): p. 313-&.
2. Bertolini, M.J., M.A. Zaghete, and R. Gimenes, *Development of an experimental glass ionomer cement containing niobium and fluoride*. Journal of Non-Crystalline Solids, 2005. **351**(52-54): p. 3884-3887.
3. Pires, R.A., C. Fernandez, and T.G. Nunes, *Structural and spatially resolved studies on the hardening of a commercial resin-modified glass-ionomer cement*. Journal of Materials Science-Materials in Medicine, 2007. **18**(5): p. 787-796.
4. Gu, Y.W. and Y.Q. Fu, *Heat treatment and thermally induced crystallization of glass for glass ionomer cement*. Thermochimica Acta, 2004. **423**(1-2): p. 107-112.
5. Kamitakahara, M., et al., *Effect of polyacrylic acid on the apatite formation of a bioactive ceramic in a simulated body fluid: fundamental examination of the possibility of obtaining bioactive glass-ionomer cements for orthopaedic use*. Biomaterials, 2001. **22**(23): p. 3191-3196.
6. Oliva, A., et al., *Biocompatibility studies on glass ionomer cements by primary cultures of human osteoblasts*. Biomaterials, 1996. **17**(13): p. 1351-1356.
7. Nakajima, H., H. Komatsu, and T. Okabe, *Aluminum ions in analysis of released fluoride from glass ionomers*. Journal of Dentistry, 1997. **25**(2): p. 137-144.
8. Brook, I.M. and P.V. Hatton, *Glass-ionomers: bioactive implant materials*. Biomaterials, 1998. **19**(6): p. 565-571.
9. Dabsie, F., et al., *Does strontium play a role in the cariostatic activity of glass ionomer?: Strontium diffusion and antibacterial activity*. Journal of Dentistry, 2009. **37**(7): p. 554-559.
10. De Barra, E. and R.G. Hill, *Influence of glass composition on the properties of glass polyalkenoate cements. Part III: influence of fluorite content*. Biomaterials, 2000. **21**(6): p. 563-569.
11. Boyce, *Toxic effect of aluminium and others substances on bone turnover*.
12. Reusche, E., et al., *Subacute fatal aluminum encephalopathy after reconstructive otoneurosurgery: A case report*. Human Pathology, 2001. **32**(10): p. 1136-1140.
13. Boyd, D., et al., *Zinc-based glass polyalkenoate cements with improved setting times and mechanical properties*. Acta Biomaterialia, 2008. **4**(2): p. 425-431.

14. Boyd, D. and M. Towler, *The processing, mechanical properties and bioactivity of zinc based glass ionomer cements*. Journal of Materials Science: Materials in Medicine, 2005. **16**(9): p. 843-850.
15. Kim, I., et al., *Fabrication of spherical CaO-SrO-ZnO-SiO_2 particles by sol-gel processing*. Journal of Materials Science: Materials in Medicine, 2009. **20**(11): p. 2267-2273.
16. Towler, M.R., C.M. Crowley, and R.G. Hill, *Investigation into the ultrasonic setting of glass ionomer cements Part I & Postulated modalities*. Journal of Materials Science Letters, 2003. **22**(7): p. 539-541.
17. Wren, A., D. Boyd, and M. Towler, *The processing, mechanical properties and bioactivity of strontium based glass polyalkenoate cements*. Journal of Materials Science: Materials in Medicine, 2008. **19**(4): p. 1737-1743.
18. Wren, A., et al., *The effect of glass synthesis route on mechanical and physical properties of resultant glass ionomer cements*. Journal of Materials Science: Materials in Medicine, 2009. **20**(10): p. 1991-1999.
19. Fennell, B. and R.G. Hill, *The influence of poly(acrylic acid) molar mass and concentration on the properties of polyalkenoate cements Part I Compressive strength*. Journal of Materials Science, 2001. **36**(21): p. 5193-5202.
20. Hill, R.G., A.D. Wilson, and C.P. Warrens, *The influence of poly(acrylic acid) molecular weight on the fracture toughness of glass-ionomer cements*. Journal of Materials Science, 1989. **24**(1): p. 363-371.
21. Brandt, B., et al., *The Influence of Particle Size on the Mechanical Properties of Dental Glass Ionomer Cements*. Advanced Engineering Materials, 2010. **12**(12): p. B684-B689.
22. Benhayoune, H.C., D.; Jallot, E.; Laquerriere, P.; Balossier, G.; Bonhomme, P., *Evaluation of the Ca/P concentration ratio in hydroxyapatite by STEM-EDXS: influence of the electron irradiation dose and temperature processing*. Journal of Physics D: Applied Physics, 2001. **34**(1): p. 141-147
23. H-M Kim, T.H., M. Kawashita, T. Kokubo, and T. Nakamura, *The mechanism of biomineralization of bone-like apatite on synthetic hydroxyapatite: an in vitro assessment*. J R Soc Interface, 2004. **1**(1): p. 17-22.

Chapter IV

General conclusions & Future
research

Aluminium-free GICs were developed through the combination of PAA, water and glass formulations of general formula $0.340\text{SiO}_2 : 0.300\text{ZnO} : (0.250 - x - y)\text{CaO} : x\text{SrO} : y\text{MgO} : 0.050\text{Na}_2\text{O} : 0.060\text{P}_2\text{O}_5$ ($x, y = 0.125$ or 0.000). Their mechanical performance was evaluated yielding compressive strengths (CS) and moduli (CM) between 11 MPa - 25 MPa and 227 MPa – 492 MPa, respectively. Highest results (CS = 25 MPa; CM = 492 MPa) were obtained with glass composition $0.340\text{SiO}_2 : 0.300\text{ZnO} : 0.125\text{CaO} : 0.125\text{SrO} : 0.050\text{Na}_2\text{O} : 0.060\text{P}_2\text{O}_5$, a glass particle size between $63\text{ }\mu\text{m} < x < 125\text{ }\mu\text{m}$ and a PAA M_w of 50 kDa.

The PAA and glass distribution within the GIC samples was studied by micro-CT, revealing that the PAA is mainly in the outer surface of the GICs while the reacted glass particles are homogeneous distributed throughout its bulk. This PAA migration to the surface of the samples may be a consequence of the pressures promoted by the moulding process. Additionally, this observation is also consistent with the higher mobility of the PAA (compared to the glass particles) within the cement paste before final curing.

The *in vitro* bioactivity of the developed GICs was evaluated by a series of techniques (ICP of the immersion SBF solutions and EDS/SEM of the cement surface before and after immersion). In all the cases they demonstrated the GICs' ability to promote the formation of a calcium phosphate layer at their surface.

Finally, in an attempt to impart biodegradability to the GICs, they were formulated with the addition of starch at weight percentages of 5% and 25%. The porosity of the developed starch containing GICs (determined by micro-CT) was in the range of 35% to 43%. Additionally, when no enzyme was used in the immersion solutions the samples' WL were similar to the control sample (0% starch), although, unexpectedly, when an enzymatic medium was used a lower WL was recorded. A possible explanation for the lower WL observed with the samples subject to enzymatic medium is related with the inhibition of the processes that induce the WL of the GICs (e.g. 0% starch). These processes might comprise the partial solubilisation of PAA and leaching of cations from the glass particles and cement matrix to the immersion solution.

Under these circumstances it was not possible to conclude about the starch containing GICs degradation from the observed WLs. In this perspective, the determination of the concentration of reducing sugars was executed and confirmed their increasing presence after 8 weeks of immersion. These results provided evidence that the starch degraded at a longer timeframe than expectable.

In general, the results showed that it is possible to formulate aluminium-free GICs with mechanical behaviour suitable to be used as bone cements in non load-bearing sites. The developed GICs presented significant bioactivity giving a good indication on their suitability for *in vitro* and/or *in vivo* testing. The inclusion of starch to the cement formulations imparted degradability in the GICs (supported by the occurrence of reducing sugars in the degradation enzymatic solution), although, the reduction of the WL when enzymatic medium was used requires further evaluation to understand the mechanisms involved in the degradation/solubilisation processes.

The work executed under this thesis resulted in promising perspectives for the biological testing of the developed GIC formulations *in vitro* and/or *in vivo*. Under this perspective it is relevant to project as future work the evaluation of their cytotoxicity. Initial *in vitro* procedure should comprise indirect contact method [1-3]. Afterwards, and still under *in vitro* testing, it is highly relevant to evaluate the suitability of the developed bone cements within similar conditions than the ones that it will face on its application site. For this purpose, it is relevant to evaluate the behavior of osteoblasts (one of the main type of cells responsible for osteogenesis) in the presence of cement specimens.

The outcome of the *in vitro* biological testing is determinant to define the following research steps. In this sense, if positive results are obtained from the *in vitro* testing, it is relevant to initiate *in vivo* testing; if negative results are obtained, the research should come back to the formulation stage with optimization of the glass composition or the polymeric part.

Another section that is opened to optimization is the PAA component. In fact, it is known that its high acidity induces pH reduction in the surrounding tissue, promoting inflammatory response. Its substitution by different types of polymeric acids is a valuable alternative that requires evaluation. Some of these

alternatives can be polysaccharide-based due to their known biocompatibility and in some cases bioactivity. Examples of these polymers are hyaluronic acid or carboxymethyl chitosan [4, 5].

The analysis of the reducing sugars, present in the degradation solution of the starch containing GICs, revealed that starch degradation only starts after the 8th week of degradation (within a 12 weeks study). In this perspective it is also relevant to test the degradability of the same starch containing GICs at a longer time frame.

Finally, the application of bone cements within the clinical domain requires strategies that enable versatility and simplicity of application to the clinician. In this perspective, it is relevant to evaluate the suitability of the developed formulations as injectable bone cement (one of the most used application systems). Under this approach, the optimization of the GIC formulation might be required in order to better control their setting time (the time that ranges from the start of mixing and the lost of cement moldability) [6-12].

Bibliography

1. Camilleri, J., *A review of the methods used to study biocompatibility of Portland cement-derived materials used in dentistry*. MMJ, 2006. **18**.
2. Schmalz, G., et al., *An in vitro pulp chamber with three-dimensional cell cultures*. Journal of Endodontics, 1999. **25**(1): p. 24-29.
3. Beltes, P., et al., *In vitro evaluation of the cytotoxicity of two glass-ionomer root canal sealers*. Journal of Endodontics, 1997. **23**(9): p. 572-574.
4. Sasaki, T. and H. Kawamata-Kido, *Providing an environment for reparative dentine induction in amputated rat molar pulp by high molecular-weight hyaluronic acid*. Archives of Oral Biology, 1995. **40**(3): p. 209-219.
5. Jin, R., et al., *Enzymatically-crosslinked injectable hydrogels based on biomimetic dextran-hyaluronic acid conjugates for cartilage tissue engineering*. Biomaterials, 2010. **31**(11): p. 3103-3113.
6. Arlsan, V., et al., *The effect of injectable calcium phosphate cement on bone anchorage of titanium implants: an experimental feasibility study in dogs*. International Journal of Oral and Maxillofacial Surgery, 2010. **39**(5): p. 463-468.
7. Larsson, S. and G. Hannink, *Injectable bone-graft substitutes: Current products, their characteristics and indications, and new developments*. Injury. **In Press, Corrected Proof**.
8. Xu, H.H.K., et al., *Injectable and macroporous calcium phosphate cement scaffold*. Biomaterials, 2006. **27**(24): p. 4279-4287.
9. Apelt, D., et al., *In vivo behavior of three different injectable hydraulic calcium phosphate cements*. Biomaterials. **25**(7-8): p. 1439-1451.
10. Gauthier, O., et al., *In vivo bone regeneration with injectable calcium phosphate biomaterial: A three-dimensional micro-computed tomographic, biomechanical and SEM study*. Biomaterials, 2005. **26**(27): p. 5444-5453.
11. Wang, X., J. Ye, and Y. Wang, *Influence of a novel radiopacifier on the properties of an injectable calcium phosphate cement*. Acta Biomaterialia, 2007. **3**(5): p. 757-763.
12. Temenoff, J.S. and A.G. Mikos, *Injectable biodegradable materials for orthopedic tissue engineering*. Biomaterials, 2000. **21**(23): p. 2405-2412.